The Convex Relaxation Barrier, Revisited: Tightened Single-Neuron Relaxations for Neural Network Verification

Christian Tjandraatmadja
Google Research
ctjandra@google.com

Ross Anderson
Google Research
rander@google.com

Joey Huchette
Rice University
joehuchette@rice.edu

Will Ma
Columbia University
wm2428@gsb.columbia.edu

Krunal Patel
Polytechnique Montréal*
krunal.patel@polymtl.ca

Juan Pablo Vielma
Google Research
jvielma@google.com

Abstract

We improve the effectiveness of propagation- and linear-optimization-based neural network verification algorithms with a new tightened convex relaxation for ReLU neurons. Unlike previous single-neuron relaxations which focus only on the univariate input space of the ReLU, our method considers the multivariate input space of the affine pre-activation function preceding the ReLU. Using results from submodularity and convex geometry, we derive an explicit description of the tightest possible convex relaxation when this multivariate input is over a box domain. We show that our convex relaxation is significantly stronger than the commonly used univariate-input relaxation which has been proposed as a natural convex relaxation barrier for verification. While our description of the relaxation may require an exponential number of inequalities, we show that they can be separated in linear time and hence can be efficiently incorporated into optimization algorithms on an as-needed basis. Based on this novel relaxation, we design two polynomial-time algorithms for neural network verification: a linear-programming-based algorithm that leverages the full power of our relaxation, and a fast propagation algorithm that generalizes existing approaches. In both cases, we show that for a modest increase in computational effort, our strengthened relaxation enables us to verify a significantly larger number of instances compared to similar algorithms.

1 Introduction

A fundamental problem in deep neural networks is to *verify* or *certify* that a trained network is *robust*, i.e. not susceptible to adversarial attacks [11, 29, 39]. Current approaches for neural network verification can be divided into *exact* (*complete*) methods and *relaxed* (*incomplete*) methods. Exact verifiers are often based on mixed integer programming (MIP) or more generally branch-and-bound [3, 4, 9, 10, 12, 14, 17, 24, 25, 31, 41, 48] or satisfiability modulo theories (SMT) [16, 19, 20, 27, 33] and, per their name, exactly solve the problem, with no false negatives or false positives. However, exact verifiers are typically based on solving NP-hard optimization problems [20] which can significantly limit their scalability. In contrast, relaxed verifiers are often based on polynomially-solvable optimization problems such as convex optimization or linear programming (LP) [2, 8, 15, 23, 26, 30, 32, 34, 47, 50], which in turn lend themselves to faster *propagation-based* methods where bounds are computed by a series of variable substitutions in a backwards pass through

*This work was completed while this author was at Google Research.

the network [36, 44, 45, 46, 49]. Unfortunately, relaxed verifiers achieve this speed and scalability by trading off effectiveness (i.e. increased false negative rates), possibly failing to certify robustness when robustness is, in fact, present. As might be expected, the success of relaxed methods hinges on their tightness, or how closely they approximate the object which they are relaxing.

As producing the tightest possible relaxation for an entire neural network is no easier than the original verification problem, most relaxation approaches turn their attention instead to simpler substructures, such as individual neurons. For example, the commonly used Δ-*relaxation*[2][16] is simple and offers the tightest possible relaxation for the univariate ReLU function, and as a result is the foundation for many relaxed verification methods. Recently, Salman et al. [32] characterized the *convex relaxation barrier*, showing that the effectiveness of all existing propagation-based fast verifiers is fundamentally limited by the tightness of this Δ-relaxation. Unfortunately, they show computationally that this convex barrier can be a severe limitation on the effectiveness of relaxed verifiers based upon it. While the convex relaxation barrier can be bypassed in various ways (e.g. considering relaxations for multiple neurons [34]), as noted in [32, Appendix A] all existing approaches that achieve this do so by trading off clarity and speed.

In this paper we improve the effectiveness of propagation- and LP-based relaxed verifiers with a new tightened convex relaxation for ReLU neurons. Unlike the Δ-relaxation which focuses only on the univariate input space of the ReLU, our relaxation considers the multivariate input space of the affine pre-activation function preceding the ReLU. By doing this, we are able to bypass the convex barrier from [32] while remaining in the realm of single-neuron relaxations that can be utilized by fast propagation- and LP-based verifiers.

More specifically, our contributions are as follows.

1. Using results from submodularity and convex geometry, we derive an explicit linear inequality description for the tightest possible convex relaxation of a single neuron, where, in the spirit of [3, 4], we take this to encompass the ReLU activation function, the affine pre-activation function preceding it, and known bounds on each input to this affine function. We show that this new convex relaxation is significantly stronger than the Δ-relaxation, and hence bypasses the convex barrier from [32] without the need to consider multi-neuron interactions as in, e.g. [34].
2. We show that this description, while requiring an exponential number of inequalities in the worst case, admits an efficient separation routine. In particular, we present a linear time algorithm that, given a point, either asserts that this point lies within the relaxation, or returns an inequality that is not satisfied by this point. Using this routine, we develop two verification algorithms that incorporate our tighter inequalities into the relaxation.
   (a) `OptC2V`: We develop a polynomial-time LP-based algorithm that harnesses the full power of our new relaxation.
   (b) `FastC2V`: We develop a fast propagation-based algorithm that generalizes existing approaches (e.g. `Fast-Lin` [44] and `DeepPoly` [36]) by dynamically adapting the relaxation using our new inequalities.
3. Computational experiments on verification problems using networks from the ERAN dataset [38] demonstrate that leveraging these inequalities yields a substantial improvement in verification capability. In particular, our fast propagation-based algorithm surpasses the strongest possible algorithm restricted by the convex barrier (i.e. optimizing over the Δ-relaxation at every neuron). We also show that our methods are competitive with more expensive state-of-the-art methods such as `RefineZono` [37] and `kPoly` [34], certifying more images than them in several cases.

2 Verification via mathematical optimization

Consider a neural network $f : \mathbb{R}^m \to \mathbb{R}^r$ described in terms of N neurons in a linear order.[3] The first m neurons are the *input neurons*, while the remaining *intermediate neurons* are indexed by

[2]Sometimes also called the *triangle relaxation* [22, 34].

[3]This allows us to consider feedforward networks, including those that skip layers (e.g. see [32, 50]).

$i = m+1, \dots, N$. Given some input $x \in \mathbb{R}^m$, the relationship $f(x) = y$ can be described as

$$\begin{aligned}
x_i &= z_i && \forall i = 1, \dots, m && \text{(the inputs)} && \text{(1a)}\\
\hat{z}_i &= \sum\nolimits_{j=1}^{i-1} w_{i,j} z_j + b_i && \forall i = m+1, \dots, N && \text{(the pre-activation value)} && \text{(1b)}\\
z_i &= \sigma(\hat{z}_i) && \forall i = m+1, \dots, N && \text{(the post-activation value)} && \text{(1c)}\\
y_i &= \sum\nolimits_{j=1}^{N} w_{i,j} z_j + b_i && \forall i = N+1, \dots, N+r && \text{(the outputs).} && \text{(1d)}
\end{aligned}$$

Here the constants w and b are the weights and biases, respectively, learned during training, while $\sigma(v) \overset{\text{def}}{=} \max\{0, v\}$ is the ReLU activation function. Appropriately, for each neuron i we dub the variable $\hat{z}_i$ the *pre-activation variable* and z_i the *post-activation variable*.

Given a trained network (i.e. fixed architecture, weights, and biases), we study a *verification problem* of the following form: given constant $c \in \mathbb{R}^r$, polyhedron $X \subseteq \mathbb{R}^m$, $\beta \in \mathbb{R}$, and

$$\gamma(c, X) \overset{\text{def}}{=} \max\nolimits_{x \in X} c \cdot f(x) \equiv \max\nolimits_{x,y,\hat{z},z} \left\{ c \cdot y \mid x \in X, \quad (1) \right\}, \tag{2}$$

does $\gamma(c, X) \leqslant \beta$? Unfortunately, this problem is NP-hard [20]. Moreover, one is typically not content with solving just one problem of this form, but would like to query for many reasonable choices of c and X to be convinced that the network is robust to adversarial perturbations.

A promising approach to approximately solving the verification problem is to replace the intractable optimization problem defining γ in (2) with a tractable *relaxation*. In particular, we aim to identify a tractable optimization problem whose optimal objective value $\gamma_R(c, X)$ satisfies $\gamma(c, X) \leqslant \gamma_R(c, X)$, for all parameters c and X of interest. Then, if $\gamma_R(c, X) \leqslant \beta$, we have answered the verification problem in the affirmative. However, note that it may well be the case that, by relaxing the problem, we may fail to verify a network that is, in fact, verifiable (i.e. $\gamma(c, X) \leqslant \beta < \gamma_R(c, X)$). Therefore, *the strength of our relaxation is crucial for reducing the false negative rate of our verification method.*

2.1 The Δ-relaxation and its convex relaxation barrier

Salman et al. [32] note that many relaxation approaches for ReLU networks are based on the single-activation-function set $A^i \overset{\text{def}}{=} \{(\hat{z}_i, z_i) \in \mathbb{R}^2 \mid \hat{L}_i \leqslant \hat{z}_i \leqslant \hat{U}_i,\ z_i = \sigma_j(\hat{z}_i)\}$, where the pre-activation bounds $\hat{L}_i, \hat{U}_i \in \mathbb{R}$ are taken so that $\hat{L}_i \leqslant \hat{z}_i \leqslant \hat{U}_i$ for any point that satisfies $x \in X$ and (1). The Δ-relaxation $C^i_\Delta \overset{\text{def}}{=} \text{Conv}(A^i)$ is optimal in the sense that it describes the convex hull of A^i, with three simple linear inequalities: $z_i \geqslant 0,\ z_i \geqslant \hat{z}_i$, and $z_i \leqslant \frac{\hat{U}_i}{\hat{U}_i - \hat{L}_i}(\hat{z}_i - \hat{L}_i)$.

The simplicity and small size of the Δ-relaxation is appealing, as it leads to the relaxation

$$\gamma_\Delta(c, X) \overset{\text{def}}{=} \max_{x,y,\hat{z},z} \left\{ c \cdot y \;\middle|\; x \in X, \quad \text{(1a)}, \text{(1b)}, \text{(1d)}, \quad (\hat{z}_i, z_i) \in C^i_\Delta \ \forall i = m+1, \dots, N \right\}. \tag{3}$$

This is a small[4] Linear Programming (LP) problem than is theoretically tractable and relatively easy to solve in practice. Moreover, a plethora of fast propagation-based algorithms [35, 36, 43, 44, 45, 49] center on an approach that can be interpreted as further relaxing γ_Δ, where inequalities describing the sets C^i_Δ are judiciously dropped from the description in such a way that this LP becomes much easier to solve. Unfortunately, Salman et al. [32] observe that the quality of the verification bounds obtained through the Δ-relaxation are intrinsically limited; a phenomenon they call the *convex relaxation barrier*. Nonetheless, this LP, along with faster propagation algorithms that utilize the inequalities defining C^i_Δ, have been frequently applied to the verification task, often with substantial success.

2.2 Our approach: Eliding pre-activation variables

In this paper, we show that we can significantly improve over the accuracy of Δ-relaxation verifiers with only a minimal trade-off in simplicity and speed. The key for this result is the observation that pre-activation variables are a "devil in disguise" in the context of convex relaxations. For a neuron i, the pre-activation variable $\hat{z}_i$ and the post-activation variable z_i form the minimal set of variables needed to capture (and relax) the nonlinearity introduced by the ReLU. However, this

[4]Here, "small" means the number of variables and constraints is $\mathcal{O}(\#$ of neurons$)$.

approach ignores the inputs to the pre-activation variable $\hat{z}_i$, i.e. the preceding post-activation variables $z_{1:i-1} \overset{\text{def}}{=} (z_1, \dots, z_{i-1})$.

Our approach captures these relationships by instead turning our attention to the i-dimensional set[5] $S^i \overset{\text{def}}{=} \left\{ z \in \mathbb{R}^i \,\middle|\, L \leqslant z_{1:i-1} \leqslant U, \quad z_i = \sigma\left(\sum_{j=1}^{i-1} w_{i,j} z_j + b_i\right) \right\}$, where the post-activation bounds $L, U \in \mathbb{R}^{i-1}$ are such that $L_j \leqslant z_j \leqslant U_j$ for each point satisfying $x \in X$ and (1). Note that no pre-activation variables appear in this description; we elide them completely, substituting the affine function describing them inside of the activation function.

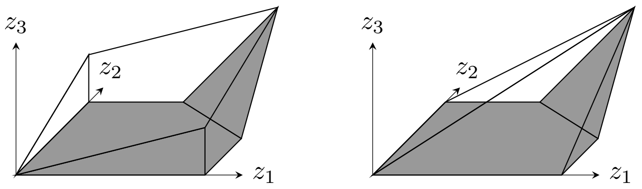

Figure 1: A simple neural network with $m = 2$ dimensional input and one intermediate neuron ($N = 3$). **(Left)** The feasible region for γ_Δ, and **(Right)** The feasible region for $\gamma_{\texttt{Elide}}$. The x, y, and $\hat{z}$ variables, which depend affinely on the others, are projected out.

This immediately gives a single-neuron relaxation of the form

$$\gamma_{\texttt{Elide}}(c, X) \overset{\text{def}}{=} \max_{x,y,z} \left\{ c \cdot y \,\middle|\, x \in X, \quad \text{(1a)}, \text{(1d)}, \quad z_{1:i} \in C^i_{\texttt{Elide}} \; \forall i = m+1, \dots, N \right\}, \tag{4}$$

where $C^i_{\texttt{Elide}} \overset{\text{def}}{=} \operatorname{Conv}(S^i)$ is the convex hull of S^i, as shown in Figure 1 (adapted from [3]), which contrasts it with the convex barrier and Δ-relaxation. We will show that, unsurprisingly, $C^i_{\texttt{Elide}}$ will require exponentially many inequalities to describe in the worst case. However, *we show that this need not be a barrier to incorporating this tighter relaxation into verification algorithms.*

3 An exact convex relaxation for a single ReLU neuron

Let $w \in \mathbb{R}^n$, $b \in \mathbb{R}$, $f(x) \overset{\text{def}}{=} w \cdot x + b$, and $L, U \in \mathbb{R}^n$ be such that $L < U$. For ease of exposition, we rewrite the single-neuron set S^i in the generic form

$$S \overset{\text{def}}{=} \{ (x, y) \in [L, U] \times \mathbb{R} \mid y = \sigma(f(x)) \}. \tag{5}$$

Notationally, take $[\![n]\!] \overset{\text{def}}{=} \{1, \dots, n\}$, $\breve{L}_i \overset{\text{def}}{=} \begin{cases} L_i & w_i \geqslant 0 \\ U_i & \text{o.w.} \end{cases}$ and $\breve{U}_i \overset{\text{def}}{=} \begin{cases} U_i & w_i \geqslant 0 \\ L_i & \text{o.w.} \end{cases}$ for each $i \in [\![n]\!]$, $\ell(I) \overset{\text{def}}{=} \sum_{i \in I} w_i \breve{L}_i + \sum_{i \notin I} w_i \breve{U}_i + b$, and

$$\mathcal{J} \overset{\text{def}}{=} \left\{ (I, h) \in 2^{[\![n]\!]} \times [\![n]\!] \,\middle|\, \ell(I) \geqslant 0, \quad \ell(I \cup \{h\}) < 0, \quad w_i \neq 0 \; \forall i \in I \right\}.$$

Our main technical result uses results from submodularity and convex geometry [1, 6, 28, 40] to give the following closed-form characterization of $\operatorname{Conv}(S)$. For a proof of Theorem 1, see Appendix A.

Theorem 1. *If* $\ell([\![n]\!]) \geqslant 0$*, then* $\operatorname{Conv}(S) = S = \{ (x, y) \in [L, U] \times \mathbb{R} \mid y = f(x) \}$*. Alternatively, if* $\ell(\varnothing) < 0$*, then* $\operatorname{Conv}(S) = S = [L, U] \times \{0\}$*. Otherwise,* $\operatorname{Conv}(S)$ *is equal to the set of all* $(x, y) \in \mathbb{R}^n \times \mathbb{R}$ *satisfying*

$$y \geqslant w \cdot x + b, \quad y \geqslant 0, \quad L \leqslant x \leqslant U \tag{6a}$$

$$y \leqslant \sum_{i \in I} w_i (x_i - \breve{L}_i) + \frac{\ell(I)}{\breve{U}_h - \breve{L}_h} (x_h - \breve{L}_h) \qquad \forall (I, h) \in \mathcal{J}. \tag{6b}$$

Furthermore, if $d \overset{\text{def}}{=} |\{ i \in [\![n]\!] \mid w_i \neq 0 \}|$*, then* $d \leqslant |\mathcal{J}| \leqslant \lceil \frac{1}{2} d \rceil \binom{d}{\lceil \frac{1}{2} d \rceil}$ *and for each of these inequalities (and each* $d \in [\![n]\!]$*) there exist data that makes it hold at equality.*

[5]The *effective* dimension of this set can be much smaller if $w_{i,\cdot}$ is sparse. This is the case with a feedforward network, where the number of nonzeros is (at most) the number of neurons in the preceding layer.

Note that this is the tightest possible relaxation when $x \in [L, U]$. Moreover, we observe that the relaxation offered by $\operatorname{Conv}(S)$ can be arbitrarily tighter than that derived from the Δ-relaxation.

Proposition 1. *For any input dimension n, there exists a point $\tilde{x} \in \mathbb{R}^n$, and a problem instance given by the affine function f, the Δ-relaxation C_Δ, and the single neuron set S such that $\left(\max_{y:(f(\tilde{x}),y)\in C_\Delta} y\right) - \left(\max_{y:(\tilde{x},y)\in \operatorname{Conv}(S)} y\right) = \Omega(n)$.*

Although the family of upper-bounding constraints (6b) may be exponentially large, the structure of the inequalities is remarkably simple. As a result, the *separation problem* can be solved efficiently: given (x, y), either verify that $(x, y) \in \operatorname{Conv}(S)$, or produce an inequality from the description (6) which is violated at (x, y). For instance, we can solve in $\mathcal{O}(n \log n)$ time the optimization problem

$$v(x) \overset{\text{def}}{=} \min \left\{ \sum\nolimits_{i\in I} w_i(x_i - \breve{L}_i) + \frac{\ell(I)}{\breve{U}_h - \breve{L}_h}(x_h - \breve{L}_h) \;\middle|\; (I, h) \in \mathcal{J} \right\}, \tag{7}$$

by sorting the indices with $w_i \neq 0$ in nondecreasing order of values $(x_i - \breve{L}_i)/(\breve{U}_i - \breve{L}_i)$, then adding them to I in this order so long as $\ell(I) \geqslant 0$ (note that adding to I can only decrease $\ell(I)$), and then letting h be the index that triggered the stopping condition $\ell(I \cup \{h\}) < 0$. For more details, see the proof of Proposition 2 in Appendix B.

Then, to check if $(x, y) \in \operatorname{Conv}(S)$, we first check if the point satisfies (6a), which can be accomplished in $\mathcal{O}(n)$ time. If so, we compute $v(x)$ in $\mathcal{O}(n \log n)$ time. If $y \leqslant v(x)$, then $(x, y) \in \operatorname{Conv}(S)$. Otherwise, an optimal solution to (7) yields an inequality from (6b) that is most violated at (x, y). In addition, we can also solve (7) slightly faster.

Proposition 2. *The optimization problem* (7) *can be solved in $\mathcal{O}(n)$ time.*

Together with the ellipsoid algorithm [18], Proposition 2 shows that the single-neuron relaxation $\gamma_{\texttt{Elide}}$ can be efficiently solved (at least in a theoretical sense).

Corollary 1. *If the weights w and biases b describing the neural network are rational, then the single-neuron relaxation* (4) *can be solved in polynomial time on the encoding sizes of w and b.*

For proofs of Proposition 1, Proposition 2 and Corollary 1, see Appendix B.

Connections with Anderson et al. [3, 4] Anderson et al. [3, 4] have previously presented a MIP formulation that exactly models the set S in (5). This formulation is *ideal* so, in particular, its LP relaxation offers a *lifted* LP formulation with one *auxiliary variable* whose projection onto the *original variables* x and y is exactly $\operatorname{Conv}(S)$. Indeed, in Appendix A.2 we provide an alternative derivation for Theorem 1 using the machinery presented in [3]. This lifted LP can be used in lieu of our new formulation (6), though it offers no greater strength and requires an additional $N - m$ variables if applied for each neuron in the network. Moreover, it is not clear how to incorporate the lifted LP into propagation-based algorithms to be presented in the following section, which naturally work in the original variable space.

4 A propagation-based algorithm

We now present a technique to use the new family of strong inequalities (6b) to generate strong post-activation bounds for a trained neural network. A step-by-step example of this method is available in Appendix D. To properly define the algorithm, we begin by restating a generic propagation-based bound generation framework under which various algorithms from the literature are special cases (partially or completely) [35, 36, 43, 44, 45, 49].

4.1 A generic framework for computing post-activation bounds

Consider a bounded input domain $X \subseteq \mathbb{R}^m$, along with a single output (i.e. $r = 1$) to be maximized, which we name $\mathcal{C}(z) = \sum_{i=1}^{\eta} c_i z_i + b$ for some $\eta \leqslant N$. In this section, our goal is produce efficient algorithms for producing valid upper bounds for $\mathcal{C}$. First, let $z_i(x)$ denote the unique value of z_i (post-activation variable i) implied by the equalities (1b–1c) when we set $z_{1:m} = x$ for some $x \in X$. Next, assume that for each intermediate neuron $i = m+1, \ldots, \eta$ we have affine functions of the form $\mathcal{L}_i(z_{1:i-1}) = \sum_{j=1}^{i-1} w^l_{ij} z_j + b^l_i$ and $\mathcal{U}_i(z_{1:i-1}) = \sum_{j=1}^{i-1} w^u_{ij} z_j + b^u_i$, such that

$$\mathcal{L}_i(z_{1:i-1}(x)) \leqslant z_i(x) \leqslant \mathcal{U}_i(z_{1:i-1}(x)) \quad \forall x \in X, \quad i = 1, \ldots, \eta. \tag{8}$$

We consider how to construct these functions in the next subsection. Then, given these functions we can compute a bound on $\mathcal{C}\left(z_{1:\eta}\left(x\right)\right)$ through the following optimization problem:

$$\begin{aligned} B\left(\mathcal{C},\eta\right) \overset{\text{def}}{=} \max_{z} \quad & \mathcal{C}(z) \equiv \sum\nolimits_{i=1}^{\eta} c_i z_i + b && \text{(9a)} \\ \text{s.t.} \quad & z_{1:m} \in X && \text{(9b)} \\ & \mathcal{L}_i(z_{1:i-1}) \leqslant z_i \leqslant \mathcal{U}_i(z_{1:i-1}) \quad \forall i = m+1,\ldots,\eta. && \text{(9c)} \end{aligned}$$

Proposition 3. *The optimal value of* (9) *is no less than* $\max_{x\in X} \mathcal{C}\left(z_{1:\eta}\left(x\right)\right)$.

The optimal value $B\left(\mathcal{C},\eta\right)$ can be quickly computed through propagation methods without explicitly computing an optimal solution to (9) [32, 49]. Such methods perform a backward pass to sequentially eliminate (project out) the intermediate variables $z_N,\ldots,z_{m+1}$, which can be interpreted as applying Fourier-Motzkin elimination [7, Chapter 2.8]. In a nutshell, for $i=\eta,\ldots,m+1$, the elimination step for variable z_i uses its objective coefficient (which may be changing throughout the algorithm) to determine which one of the bounds from (9c) will be binding at the optimal solution and replaces z_i by the expression $\mathcal{L}_i(z_{1:i-1})$ or $\mathcal{U}_i(z_{1:i-1})$ accordingly. The procedure ends with a smaller LP that only involves the input variables $z_{1:m}$ and can be quickly solved with an appropriate method. For instance, when X is a box, as is common in verification problems, this final LP can be trivially solved by considering each variable individually. For more details, see Algorithm 1 in Appendix C.

4.2 Selecting the bounding functions

The framework described in the previous section required as input the family of bounding functions $\{\mathcal{L}_i,\mathcal{U}_i\}_{i=m+1}^{\eta}$. A typical approach to generate these will proceed sequentially, deriving the i-th pair of functions using *scalar bounds* $\hat{L}_i,\hat{U}_i \in \mathbb{R}$ on the i-th pre-activation variables $\hat{z}_i$, which by (1b) is equal to $\sum_{j=1}^{i-1} w_{i,j}z_j + b_i$. Hence, these scalar bounds must satisfy

$$\hat{L}_i \leqslant \sum\nolimits_{j=1}^{i-1} w_{i,j}z_j(x) + b_i \leqslant \hat{U}_i \quad \forall x \in X. \tag{10}$$

These bounds can then be used as a basis to linearize the nonlinear equation

$$z_i = \sigma\left(\sum\nolimits_{j=1}^{i-1} w_{i,j}z_j + b_i\right) \tag{11}$$

implied by (1b-1c). If $\hat{U}_i \leqslant 0$ or $\hat{L}_i \geqslant 0$, then (11) behaves linearly when (10) holds, and so we can let $\mathcal{L}_i(z_{1:i-1}) = \mathcal{U}_i(z_{1:i-1}) = \sum_{j=1}^{i-1} w_{i,j}z_j + b_i$ or $\mathcal{L}_i(z_{1:i-1}) = \mathcal{U}_i(z_{1:i-1}) = 0$, respectively. Otherwise, we can construct non-trivial bounds such as

$$\mathcal{L}_i(z_{1:i-1}) = \frac{\hat{U}_i}{\hat{U}_i - \hat{L}_i}\left(\sum_{j=1}^{i-1} w_{i,j}z_j + b_i\right) \quad \text{and} \quad \mathcal{U}_i(z_{1:i-1}) = \frac{\hat{U}_i}{\hat{U}_i - \hat{L}_i}\left(\sum_{j=1}^{i-1} w_{i,j}z_j + b_i - \hat{L}_i\right),$$

which can be derived from the Δ-relaxation: $\mathcal{U}_i(z_{1:i-1})$ is the single upper-bounding inequality present on the left side of Figure 1, and $\mathcal{L}_i(z_{1:i-1})$ is a shifted down version of this inequality.[6] This pair is used by algorithms such as `Fast-Lin` [44], `DeepZ` [35], `Neurify` [43], and that of Wong and Kolter [45]. Algorithms such as `DeepPoly` [36] and `CROWN-Ada` [49] can be derived by selecting the same $\mathcal{U}_i(z_{1:i-1})$ as above and $\mathcal{L}_i(z_{1:i-1}) = 0$ if $|\hat{L}_i| \geqslant |\hat{U}_i|$ or $\mathcal{L}_i(z_{1:i-1}) = \sum_{j=1}^{i-1} w_{i,j}z_j + b_i$ otherwise (i.e. whichever yields the smallest area of the relaxation). In the next subsection, we propose using (6b) for $\mathcal{U}_i(z_{1:i-1})$.

Scalar bounds satisfying (10) for the i-th pre-activation variable can be computed by letting $\mathcal{C}^{U,i}\left(z_{1:(i-1)}\right) = \sum_{j=1}^{i-1} w_{i,j}z_j + b_i$ and then setting $\hat{L}_i = -B\left(\mathcal{C}^{L,i}, i-1\right)$ and $\hat{U}_i = B\left(\mathcal{C}^{U,i}, i-1\right)$. Therefore, to reach a final bound for $\eta = N$, we can iteratively compute $\hat{L}_i$ and $\hat{U}_i$ for $i = m+1,\ldots,N$ by solving (9) each time, since each of these problems requires only affine bounding functions up to intermediate neuron $i-1$. See Algorithm 4 in Appendix C for details.

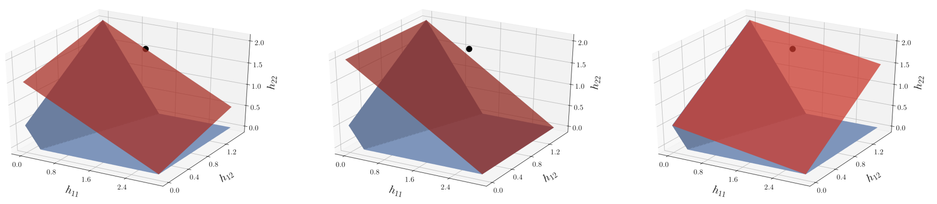

(a) An inequality from the Δ-relaxation. (b) An inequality from (6b). (c) Another inequality from (6b).

Figure 2: Possible choices of upper bounding functions $\mathcal{U}_i$ for a single ReLU. The black point depicts a solution $z_{1:N}$ that we would like to separate (projected to the input-output space of the ReLU), which is cut off by the inequality in (b). A full example involving these particular inequalities can be found in Appendix D.

4.3 Our contribution: Tighter bounds by dynamically updating bounding functions

In Theorem 1 we have derived a family of inequalities, (6b), which can be applied to yield valid upper bounding affine functions for each intermediate neuron in a network. As there may be exponentially many such inequalities, it is not clear *a priori* which to select as input to the algorithm from Section 4.1. Therefore, we present a simple iterative scheme in which we apply a small number of solves of (9), incrementally updating the set of affine bounding functions used at each iteration.

Our goal is to update the upper bounding function $\mathcal{U}_i$ with one of the inequalities from (6b) as illustrated in Figure 2 via the separation procedure of Proposition 2, which requires an optimal solution $z_{1:N}$ for (9). However, the backward pass of the propagation algorithm described in Section 4.1 only computes the optimal value $B(\mathcal{C}, \eta)$ and a partial solution $z_{1:m}$. For this reason, we first extend the propagation algorithm with a forward pass that completes the partial solution $z_{1:m}$ by propagating the values for $z_{m+1}, \ldots, z_N$ through the network. This propagation uses the same affine bounding functions from (9c) that were used to eliminate variables in the backward pass. For more details, see Algorithm 2 in Appendix C.

In essence, our complete dynamic algorithm initializes with a set of bounding functions (e.g. from `Fast-Lin` or `DeepPoly`), applies a backward pass to solve the bounding problem, and then a forward pass to reconstruct the full solution. It then takes that full solution, and at each intermediate neuron i applies the separation procedure of Proposition 2 to produce an inequality from the family (6b). If this inequality is violated, it replaces the upper bounding function $\mathcal{U}_i$ with this inequality from (6b). We repeat for as many iterations as desired and take the best bound produced across all iterations. In this way, we use separation to help us select from a large family just one inequality that will (hopefully) be most beneficial for improving the bound. For more details, see Algorithm 3 in Appendix C.

5 Computational experiments

5.1 Computational setup

We evaluate two methods: the propagation-based algorithm from Section 4.3 and a method based on partially solving the LP from Theorem 1 by treating the inequalities (6b) as cutting planes, i.e. inequalities that are dynamically added to tighten a relaxation. To focus on the benefit of incorporating the inequalities (6b) into verification algorithms, we implement simple versions of the algorithms, devoid of extraneous features and fine-tuning. We name this framework "Cut-to-Verify" (C2V), and the propagation-based and LP-based algorithms `FastC2V` and `OptC2V`, respectively. See `https://github.com/google-research/tf-opt` for the implementation.

The overall framework in both methods is the same: we compute scalar bounds for the pre-activation variables of all neurons as we move forward in the network, using those bounds to produce the subsequent affine bounding functions and LP formulations as discussed in Section 4.2. Below, we describe the bounds computation for each individual neuron.

[6]Note that these functions satisfy (8) only when $\hat{U}_i > 0$ and $\hat{L}_i < 0$.

Propagation-based algorithm (`FastC2V`). We implement the algorithm described in Section 4.3, using the initial affine bounding functions $\{\mathcal{L}_i, \mathcal{U}_i\}_{i=m+1}^{N}$ from `DeepPoly` [36] and `CROWN-Ada` [49], as described in Section 4.1.[7] In this implementation, we run a single iteration of the algorithm.

LP-based algorithm (`OptC2V`). Each bound is generated by solving a series of LPs where our upper bounding inequalities are dynamically generated and added as cutting planes. We start with the standard Δ-relaxation LP, solve it to optimality, and then for every neuron preceding the one we are bounding, we add the most violated inequality with respect to the LP optimum by solving (7). This can be repeated multiple times. In this implementation, we perform three rounds of separation. We generate new cuts from scratch for each bound that we compute.

In both methods, at each neuron we take the best between the bound produced by the method and the trivial interval arithmetic bound. Appendix E contains other implementation details.

We compare each of our novel algorithms against their natural baselines: `DeepPoly` for our propagation-based method, and the standard Δ-relaxation LP for our cutting plane method. Our implementation of `DeepPoly` is slightly different from the one in [36] in that we take the best of interval arithmetic and the result of `DeepPoly` at each neuron. Moreover, our implementation is sequential, even though operations in the same layer could be parallelized (for each of the algorithms implemented in this work). The LP method simply solves the Δ-relaxation LP to generate bounds at each neuron. In addition, we compare them with `RefineZono` [37] and `kPoly` [34], two state-of-the-art incomplete verification methods.

Verification problem. We consider the following verification problem: given a correctly labeled target image, certify that the neural network returns the same label for each input within L_∞-distance at most ϵ of that target image. More precisely, given an image $\hat{x} \in [0,1]^m$ correctly labeled as t, a neural network where $f_k(x)$ returns its logit for class $k \in K$, and a distance $\epsilon > 0$, the image $\hat{x}$ is verified to be robust if $\max_{x \in [\hat{L}, \hat{U}]} \max_{k \in K} \{f_k(x) - f_t(x)\} < 0$, where $\hat{L}_i = \max\{0, \hat{x}_i - \epsilon\}$ and $\hat{U}_i = \min\{1, \hat{x}_i + \epsilon\}$ for all $i = 1, \ldots, m$. For propagation-based methods, the inner $\max$ term can be handled by computing bounds for $f_k(x) - f_t(x)$ for every class $k \neq t$ and checking if the maximum bound is negative, although we only need to compute pre-activation bounds throughout the network once. For LP-based methods, this inner term can be incorporated directly into the model.

To facilitate the comparison with existing algorithms, our experimental setup closely follows that of Singh et al. [34]. We experiment on a subset of trained neural networks from the publicly available ERAN dataset [38]. We examine the following networks: the fully connected ReLU networks 6x100 ($\epsilon = 0.026$), 9x100 ($\epsilon = 0.026$), 6x200 ($\epsilon = 0.015$), 9x200 ($\epsilon = 0.015$), all trained on MNIST without adversarial training; the ReLU convolutional networks ConvSmall for MNIST ($\epsilon = 0.12$), with 3 layers and trained without adversarial training; the ReLU network ConvBig for MNIST ($\epsilon = 0.3$), with 6 layers and trained with DiffAI; and the ReLU network ConvSmall for CIFAR-10 ($\epsilon = 2/255$), with 3 layers and trained with PGD. These ϵ values are the ones used in [34] and they are cited as being challenging. For more details on these networks, see Appendix E or [38]. For each network, we verify the first 1000 images from their respective test sets except those that are incorrectly classified.

Due to numerical issues with LPs, we zero out small values in the convolutional networks for the LP-based algorithms (see Appendix E). Other than this, we do not perform any tuning according to instance. Our implementation is in C++ and we perform our experiments in an Intel Xeon E5-2699 2.3Ghz machine with 128GB of RAM. We use Gurobi 8.1 as the LP solver, take advantage of incremental solves, and set the LP algorithm to dual simplex, as we find it to be faster for these LPs in practice. This means that our LP implementation does not run in polynomial time, even though it could in theory by using a different LP algorithm (see Corollary 1).

To contextualize the results, we include an upper bound on the number of verifiable images. This is computed with a standard implementation of gradient descent with learning rate 0.01 and 20 steps. For each image, we take 100 random initializations (10 for MNIST ConvBig and CIFAR-10 ConvSmall) and check if the adversarial example produced by gradient descent is valid. The upper bound is the number of images for which we were unable to produce an adversarial example.

[7] Our framework supports initializing from the `Fast-Lin` inequalities as well, but it has been observed that the inequalities from `DeepPoly` perform better computationally.

Table 1: Number of images verified and average verification times per image for a set of networks from the ERAN dataset [38]. ConvS and ConvB denote ConvSmall and ConvBig, respectively. Results for `RefineZono` and `kPoly` are taken from [34].

		MNIST						CIFAR-10
Method		6x100	9x100	6x200	9x200	ConvS	ConvB	ConvS
`DeepPoly`	#verified	160	182	292	259	162	652	359
	Time (s)	0.7	1.4	2.4	5.6	0.9	7.4	2.8
`FastC2V`	#verified	279	269	477	392	274	691	390
	Time (s)	8.7	19.3	25.2	57.2	5.3	16.3	15.3
`LP`	#verified	201	223	344	307	242	743	373
	Time (s)	50.5	385.6	218.2	2824.7	23.1	24.9	38.1
`OptC2V`	#verified	429	384	601	528	436	771	398
	Time (s)	136.7	759.4	402.8	3450.7	55.4	102.0	104.8
`RefineZono`	#verified	312	304	341	316	179	648	347
`kPoly`	#verified	441	369	574	506	347	736	399
Upper bound	#verified	842	820	901	911	746	831	482

5.2 Computational results

The computational results in Table 1 demonstrate that adding the upper bounding inequalities proposed in this paper significantly improves the number of images verified compared to their base counterparts. While on average `FastC2V` spends an order of magnitude more time than `DeepPoly` to achieve this, it still takes below one minute on average for all instances examined. `OptC2V` takes approximately 1.2 to 2.7 times of a pure LP method to generate bounds in the problems examined. Since we start from the LP basis of the previous solve, subsequent LPs after adding cuts are generally faster.

Interestingly, we observe that `FastC2V` verifies more images than LP in almost all cases in much less time. This indicates that, in practice, a two-inequality relaxation with a single (carefully chosen) tighter inequality from (6b) can often be stronger than the three-inequality Δ-relaxation.

When compared to other state-of-the-art incomplete verifiers, we observe that for the larger networks, improving `DeepPoly` with our inequalities enables it to verify more images than `RefineZono` [37], a highly fine-tuned method that combines MIP, LP, and `DeepPoly`, but without the expensive computation and the parameter tuning needs from `RefineZono`. In addition, we find that adding our inequalities to LPs is competitive with `kPoly`, surpassing it for some of the networks. While the timings in [34] may not be comparable to our timings, the authors report average times for `RefineZono` and `kPoly` within the range of 4 to 15 minutes and 40 seconds to 8 minutes, respectively.

Appendix F contains additional computational results where we consider multiple trained networks and distances ϵ from the base image.

Outlook: Our methods as subroutines The scope of our computational experiments is to demonstrate the practicality and strength of our full-neuron relaxation applied to simple methods, rather than to engineer full-blown state-of-the-art verification methods. Towards such a goal, we remark that both `RefineZono` and `kPoly` rely on LP and other faster verification methods as building blocks to a stronger method, and either of our methods could be plugged into them. For example, we could consider a hybrid approach similar to `RefineZono` that uses the stronger, but slower `OptC2V` in the earlier layers (where it can have the most impact) and then switches to `FastC2V`, which could result in verification times closer to `FastC2V` with an effectiveness closer to `OptC2V`. In addition, `kPoly` exploits the correlation between multiple neurons in the same layer, whereas our approach does not, suggesting that there is room to combine approaches. Finally, we note that solving time can be controlled with a more careful management of the inequalities to be added and parallelizing bound computation of neurons in the same layer.

Broader Impact

In a world where deep learning is impacting our lives in ever more tangible ways, verification is an essential task to ensure that these black box systems behave as we expect them to. Our fast, simple algorithms have the potential to make a positive impact by verifying a larger number of inputs to be robust within a short time-frame, often required in several applications. Of course, we should be cautious that although our algorithms provide a mathematical certificate of an instance being robust, failure to use the system correctly, such as modeling the verification problem in a way that does not reflect real-world concerns, can still lead to unreliable neural networks. We also highlight that our version of the verification problem, while accurately capturing a reasonable formal specification of robustness, clearly does not perfectly coincide with "robustness" as may be used in a colloquial sense. Therefore, we highlight the importance of understanding the strengths and limitations of the mathematical model of verification used, so that a false sense of complacency does not set in.

Funding Disclosure

No third-party funding was received for this work.

References

[1] Shabbir Ahmed and Alper Atamtürk. Maximizing a class of submodular utility functions. *Mathematical programming*, 128(1-2):149–169, 2011.

[2] Brendon G Anderson, Ziye Ma, Jingqi Li, and Somayeh Sojoudi. Tightened convex relaxations for neural network robustness certification. *arXiv preprint arXiv:2004.00570*, 2020.

[3] Ross Anderson, Joey Huchette, Will Ma, Christian Tjandraatmadja, and Juan Pablo Vielma. Strong mixed-integer programming formulations for trained neural networks. *Mathematical Programming*, pages 1–37, 2020.

[4] Ross Anderson, Joey Huchette, Christian Tjandraatmadja, and Juan Pablo Vielma. Strong mixed-integer programming formulations for trained neural networks. In A. Lodi and V. Nagarajan, editors, *Proceedings of the 20th Conference on Integer Programming and Combinatorial Optimization (IPCO 2019)*, volume 11480 of *Lecture Notes in Computer Science*, pages 27–42, 2019.

[5] Martin Anthony. *Discrete mathematics of neural networks: selected topics*, volume 8. SIAM, 2001.

[6] Francis Bach. Learning with submodular functions: A convex optimization perspective. *Foundations and Trends® in Machine Learning*, 6(2-3):145–373, 2013.

[7] Dimitris Bertsimas and John Tsitsiklis. *Introduction to Linear Optimization*. Athena Scientific, 1997.

[8] Srinadh Bhojanapalli, Rudy Bunel, Krishnamurthy Dvijotham, and Oliver Hinder. An efficient nonconvex reformulation of stagewise convex optimization problems. In *Advances in Neural Information Processing Systems*, 2020.

[9] Elena Botoeva, Panagiotis Kouvaros, Jan Kronqvist, Alessio Lomuscio, and Ruth Misener. Efficient verification of ReLU-based neural networks via dependency analysis. In *Thirty-Fourth AAAI Conference on Artificial Intelligence*, 2020.

[10] Rudy Bunel, Jingyue Lu, Ilker Turkaslan, P Kohli, P Torr, and P Mudigonda. Branch and bound for piecewise linear neural network verification. *Journal of Machine Learning Research*, 21(2020), 2020.

[11] Nicholas Carlini and David Wagner. Towards evaluating the robustness of neural networks. In *2017 IEEE Symposium on Security and Privacy (SP)*, pages 39–57, 2017.

[12] Chih-Hong Cheng, Georg Nührenberg, and Harald Ruess. Maximum resilience of artificial neural networks. In *International Symposium on Automated Technology for Verification and Analysis*, pages 251–268. Springer, 2017.

[13] Michele Conforti, Gérard Cornuéjols, and Giacomo Zambelli. *Integer programming*, volume 271. Springer, 2014.

[14] Souradeep Dutta, Susmit Jha, Sriram Sankaranarayanan, and Ashish Tiwari. Output range analysis for deep feedforward neural networks. In *NASA Formal Methods Symposium*, pages 121–138. Springer, 2018.

[15] Krishnamurthy Dvijotham, Robert Stanforth, Sven Gowal, Timothy A Mann, and Pushmeet Kohli. A dual approach to scalable verification of deep networks. In *UAI*, volume 1, page 2, 2018.

[16] Ruediger Ehlers. Formal verification of piece-wise linear feed-forward neural networks. In *International Symposium on Automated Technology for Verification and Analysis*, pages 269–286. Springer, 2017.

[17] Matteo Fischetti and Jason Jo. Deep neural networks as 0-1 mixed integer linear programs: A feasibility study. *Constraints*, 23:296–309, 2018.

[18] Martin Grötschel, László Lovász, and Alexander Schrijver. *Geometric algorithms and combinatorial optimization*, volume 2. Springer Science & Business Media, 2012.

[19] Xiaowei Huang, Marta Kwiatkowska, Sen Wang, and Min Wu. Safety verification of deep neural networks. In *International Conference on Computer Aided Verification*, pages 3–29. Springer, 2017.

[20] Guy Katz, Clark Barrett, David L. Dill, Kyle Julian, and Mykel J. Kochenderfer. Reluplex: An efficient SMT solver for verifying deep neural networks. In *International Conference on Computer Aided Verification*, pages 97–117, 2017.

[21] Bernhard Korte and Jens Vygen. *Combinatorial Optimization: Theory and Algorithms*. Springer, 2000.

[22] Changliu Liu, Tomer Arnon, Christopher Lazarus, Clark Barrett, and Mykel J Kochenderfer. Algorithms for verifying deep neural networks. *arXiv preprint arXiv:1903.06758*, 2019.

[23] Chen Liu, Mathieu Salzmann, and Sabine Süsstrunk. Training provably robust models by polyhedral envelope regularization. *arXiv*, pages arXiv–1912, 2019.

[24] Alessio Lomuscio and Lalit Maganti. An approach to reachability analysis for feed-forward ReLU neural networks. *arXiv preprint arXiv:1706.07351*, 2017.

[25] Jingyue Lu and M. Pawan Kumar. Neural network branching for neural network verification. In *International Conference on Learning Representations*, 2020.

[26] Zhaoyang Lyu, Ching-Yun Ko, Zhifeng Kong, Ngai Wong, Dahua Lin, and Luca Daniel. Fastened CROWN: Tightened neural network robustness certificates. *arXiv preprint arXiv:1912.00574*, 2019.

[27] Nina Narodytska, Shiva Kasiviswanathan, Leonid Ryzhyk, Mooly Sagiv, and Toby Walsh. Verifying properties of binarized deep neural networks. In *Thirty-Second AAAI Conference on Artificial Intelligence*, 2018.

[28] Patrick E O'Neil. Hyperplane cuts of an n-cube. *Discrete Mathematics*, 1(2):193–195, 1971.

[29] Nicolas Papernot, Patrick McDaniel, Somesh Jha, Matt Fredrikson, Z. Berkay Celik, and Ananthram Swami. The limitations of deep learning in adversarial settings. In *IEEE European Symposium on Security and Privacy*, pages 372–387, March 2016.

[30] Aditi Raghunathan, Jacob Steinhardt, and Percy S Liang. Semidefinite relaxations for certifying robustness to adversarial examples. In *Advances in Neural Information Processing Systems*, pages 10877–10887, 2018.

[31] Ansgar Rössig. Verification of neural networks. Technical Report 19-40, ZIB, Takustr. 7, 14195 Berlin, 2019.

[32] Hadi Salman, Greg Yang, Huan Zhang, Cho-Jui Hsieh, and Pengchuan Zhang. A convex relaxation barrier to tight robustness verification of neural networks. In *Advances in Neural Information Processing Systems*, pages 9832–9842, 2019.

[33] Karsten Scheibler, Leonore Winterer, Ralf Wimmer, and Bernd Becker. Towards verification of artificial neural networks. In *MBMV*, pages 30–40, 2015.

[34] Gagandeep Singh, Rupanshu Ganvir, Markus Püschel, and Martin Vechev. Beyond the single neuron convex barrier for neural network certification. In *Advances in Neural Information Processing Systems*, pages 15072–15083, 2019.

[35] Gagandeep Singh, Timon Gehr, Matthew Mirman, Markus Püschel, and Martin Vechev. Fast and effective robustness certification. In *Advances in Neural Information Processing Systems*, pages 10802–10813, 2018.

[36] Gagandeep Singh, Timon Gehr, Markus Püschel, and Martin Vechev. An abstract domain for certifying neural networks. *Proceedings of the ACM on Programming Languages*, 3(POPL):1–30, 2019.

[37] Gagandeep Singh, Timon Gehr, Markus Püschel, and Martin Vechev. Boosting robustness certification of neural networks. In *International Conference on Learning Representations*, 2019.

[38] Gagandeep Singh, Jonathan Maurer, Christoph Müller, Matthew Mirman, Timon Gehr, Adrian Hoffmann, Petar Tsankov, Dana Drachsler Cohen, Markus Püschel, and Martin Vechev. ERAN verification dataset. `https://github.com/eth-sri/eran`.

[39] Christian Szegedy, Wojciech Zaremba, Ilya Sutskever, Joan Bruna, Dumitru Erhan, Ian Goodfellow, and Rob Fergus. Intriguing properties of neural networks. In *International Conference on Learning Representations*, 2014.

[40] Mohit Tawarmalani, Jean-Philippe P Richard, and Chuanhui Xiong. Explicit convex and concave envelopes through polyhedral subdivisions. *Mathematical Programming*, 138(1-2):531–577, 2013.

[41] Vincent Tjeng, Kai Xiao, and Russ Tedrake. Verifying neural networks with mixed integer programming. In *International Conference on Learning Representations*, 2019.

[42] M.J. Todd. *The Computation of Fixed Points and Applications*. Lecture Notes in Mathematics; 513. Springer-Verlag, 1976.

[43] Shiqi Wang, Kexin Pei, Justin Whitehouse, Junfeng Yang, and Suman Jana. Efficient formal safety analysis of neural networks. In *Advances in Neural Information Processing Systems*, pages 6367–6377, 2018.

[44] Lily Weng, Huan Zhang, Hongge Chen, Zhao Song, Cho-Jui Hsieh, Luca Daniel, Duane Boning, and Inderjit Dhillon. Towards fast computation of certified robustness for ReLU networks. In Jennifer Dy and Andreas Krause, editors, *Proceedings of the 35th International Conference on Machine Learning*, volume 80 of *Proceedings of Machine Learning Research*, pages 5276–5285, Stockholmsmässan, Stockholm Sweden, 10–15 Jul 2018. PMLR.

[45] Eric Wong and J. Zico Kolter. Provable defenses against adversarial examples via the convex outer adversarial polytope. In *International Conference on Machine Learning*, pages 5286–5295, 2018.

[46] Eric Wong, Frank Schmidt, Jan Hendrik Metzen, and J. Zico Kolter. Scaling provable adversarial defenses. In *32nd Conference on Neural Information Processing Systems*, 2018.

[47] Weiming Xiang, Hoang-Dung Tran, and Taylor T Johnson. Output reachable set estimation and verification for multilayer neural networks. *IEEE Transactions on Neural Networks and Learning Systems*, 29(11):5777–5783, 2018.

[48] Kai Y. Xiao, Vincent Tjeng, Nur Muhammad Shafiullah, and Aleksander Madry. Training for faster adversarial robustness verification via inducing ReLU stability. In *International Conference on Learning Representations*, 2019.

[49] Huan Zhang, Tsui-Wei Weng, Pin-Yu Chen, Cho-Jui Hsieh, and Luca Daniel. Efficient neural network robustness certification with general activation functions. In *Advances in neural information processing systems*, pages 4939–4948, 2018.

[50] Chen Zhu, Renkun Ni, Ping-yeh Chiang, Hengduo Li, Furong Huang, and Tom Goldstein. Improving the tightness of convex relaxation bounds for training certifiably robust classifiers. *arXiv preprint arXiv:2002.09766*, 2020.

A Proof of Theorem 1

We provide two different proofs for Theorem 1. The first proof is based on classical machinery from submodular and convex optimization. The alternative proof is based on projecting down an extended MIP formulation built using disjunctive programming. We include them both since each proof provides unique insights on our new relaxation.

We first state a lemma that is used by both proofs for bounding the number of inequalities. Notationally, we will take $\mathbf{0}^d$ and $\mathbf{1}^d$ as the length d vectors of all zeros and all ones, respectively, and $e(i) \in \mathbb{R}^n$ for $i \in [\![n]\!]$ as the i-th canonical unit vector, where the length will be implicitly determined by the context of its use. In some cases it will be convenient to refer to the 0-th canonical vector $e(0) = \mathbf{0}^n$.

Lemma 1. *If $u, v \in \{0,1\}^d$ are such that $\sum_{i=1}^d |u_i - v_i| = 1$, then we say that uv is an edge of $[0,1]^d$. For $w \in \mathbb{R}^d$ and $b \in \mathbb{R}$, we say the hyperplane $w \cdot x + b = 0$ cuts edge uv of $[0,1]^d$ if $w \cdot u + b < 0$ and $w \cdot v + b \geqslant 0$. If $b < 0$ and $\sum_{i=1}^d w_i + b \geqslant 0$, then the number of edges cut by one such hyperplane is lower-bounded by d and upper-bounded by $\lceil \frac{1}{2} d \rceil \binom{d}{\lceil \frac{1}{2} d \rceil}$. For each bound there exists a hyperplane with $w \in \mathbb{R}^d_+$ such that the bounds holds at equality.*

Proof. Consider the graph $G = (V, E)$ with $V = \{0,1\}^d$ and E equal to the edges of $[0,1]^d$. Let $s = \mathbf{0}^d$ and $t = \mathbf{1}^d$. Then $w \cdot s + b < 0$ and $w \cdot t + b \geqslant 0$, so the edges of $[0,1]^d$ cut by the hyperplane form a $s - t$ graph-cut in G (note that this does *not* have the same meaning as the definition of cut for an edge given in the Lemma statement). Hence, the number of edges cut by the hyperplane are lower bounded by d (e.g. follows by Menger's theorem by noting that there are d disjoint paths in G from s to t). An example of a hyperplane that achieves this lower bound is $w = \mathbf{1}^d$ and $b = -1/2$.

The tight upper bound follows from a simple adaptation of the proof of a result from [28].[8] An example of a hyperplane that achieves this upper bound is $w = \mathbf{1}^d$ and $b = -\lceil \frac{1}{2} d \rceil$. □

A.1 A proof using submodularity

We start with an example.

A.1.1 Illustrative example and definitions

Example 1. *Consider the set from (5) for $n = 2$, $w = (1,1)$, $b = (-1.5)$, $L = (0,0)$ and $U = (0,0)$, which corresponds to*

$$S = \left\{ (x,y) \in [0,1]^2 \times \mathbb{R} \;\middle|\; y = g(x) \right\}$$

for $g(x) \overset{\text{def}}{=} \max\{0, x_1 + x_2 - 1.5\}$. Set S is depicted in Figure 3 and we can check that $\operatorname{Conv}(S)$ is described by

$$x \in [0,1]^2 \tag{12a}$$

$$y \geqslant g(x) \tag{12b}$$

$$y \leqslant r_1(x), \quad y \leqslant r_2(x) \tag{12c}$$

for $r_1(x) \overset{\text{def}}{=} 0.5x_2$ and $r_2(x) \overset{\text{def}}{=} 0.5x_1$. Inequality (12b) is obtained by relaxing the equation describing S to an inequality and using the fact that $g(x)$ is convex. Functions r_1 and r_2 from inequality (12c) are depicted in Figures 3a and 3b, respectively. These functions can be obtained through the following interpolation procedure.

First, consider the subdivision of $[0,1]^2$ into the triangles $\mathbf{T}_1$ and $\mathbf{T}_2$ depicted in Figures 3a and 3b, respectively. As depicted Figure 3a, the vertices of $\mathbf{T}_1$ are obtained by incrementally adding the canonical vectors to $(0,0)$, in order, until we obtain $(1,1)$. That is, the vertices of $\mathbf{T}_1$ are $e(0) = (0,0)$, $e(0) + e(1) = e(1) = (0,1)$ and $e(0) + e(1) + e(2) = (1,1)$. In contrast, as depicted in Figure 3b, the vertices of $\mathbf{T}_2$ are obtained by incrementally adding the canonical vectors in reverse order (i.e. the vertices of $\mathbf{T}_2$ are $e(0) = (0,0)$, $e(0) + e(2) = (1,0)$ and $e(0) + e(2) + e(1) = (1,1)$).

[8] See also [5, Theorem 7.9]: the proof of [28, Lemma 2] can be readily adapted to accommodate non-strict, rather than strict, linear inequalities.

Second, we obtain r_1 and r_2 by constructing the unique affine interpolation of g on $\mathbf{T}_1$ and $\mathbf{T}_2$, respectively. That is, as depicted in Figure 3a, $r_1(x) = \alpha^1 \cdot x + \beta_1$, where $\alpha^1 \in \mathbb{R}^2$ and $\beta_1 \in \mathbb{R}$ are such that r_1 is equal to g for the three vertices $(0,0)$, $(1,0)$ and $(1,1)$ of $\mathbf{T}_1$:

$$\begin{pmatrix} 0 & 0 \\ 1 & 0 \\ 1 & 1 \end{pmatrix} \alpha^1 + \beta_1 = \begin{pmatrix} g(0,0) \\ g(1,0) \\ g(1,1) \end{pmatrix} = \begin{pmatrix} 0 \\ 0 \\ 0.5 \end{pmatrix}.$$

The unique solution of this system is $\alpha^1 = (0, 0.5)$ and $\beta_1 = 0$, which yields $r_1(x) = 0.5x_2$. Function r_2 is obtained by a similar procedure using the vertices of $\mathbf{T}_2$ as illustrated Figure 3b.

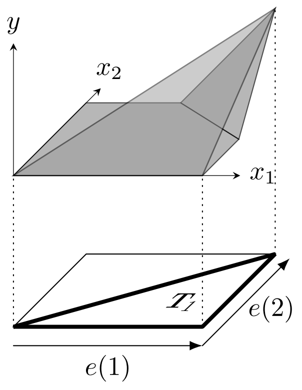

(a) Constructing r_1 using $\mathbf{T}_1$.

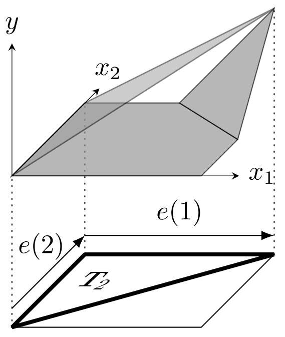

(b) Constructing r_2 using $\mathbf{T}_2$.

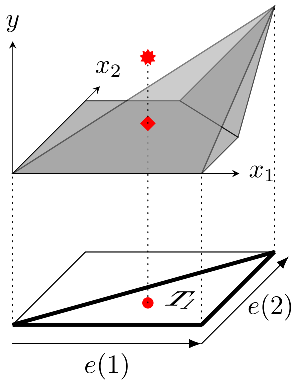

(c) Checking membership in $\mathrm{Conv}(S)$.

Figure 3: Using interpolation on triangles to construct $\mathrm{Conv}(S)$ for Example 1.

The subdivision of $[0,1]^2$ into $\mathbf{T}_1$ and $\mathbf{T}_2$ can be extended to $[0,1]^n$ by considering all $n!$ possible orders in which we can obtain $\mathbf{1}^n$ from $\mathbf{0}^n$ by incrementally adding the canonical vectors. We represent these orders using the set of all permutations of $[\![n]\!]$. In Example 1, this set is given by $\mathcal{S}_2 \overset{\text{def}}{=} \{ \pi_1, \pi_2 \}$, where $\pi_i : [\![2]\!] \to [\![2]\!]$ for each $i \in [\![2]\!]$, $\pi_1(1) = 1$, $\pi_1(2) = 2$, $\pi_2(1) = 2$, and $\pi_2(2) = 1$. Then, under the notation of Definition 1 below, we have $\mathbf{T}_1 = \mathbf{T}_{\pi_1}$ and $\mathbf{T}_2 = \mathbf{T}_{\pi_2}$.

Definition 1. *Let $\mathcal{S}_n$ be the set of all permutations of $[\![n]\!]$. Then for every $\pi \in \mathcal{S}_n$, we define $\mathbf{V}_\pi = \left\{ \sum_{i=0}^{j} e(\pi(i)) \right\}_{j=0}^{n}$ and*

$$\mathbf{T}_\pi = \mathrm{conv}\left(\mathbf{V}_\pi\right) = \left\{ x \in \mathbb{R}^n \;\middle|\; 1 \geqslant x_{\pi(1)} \geqslant x_{\pi(2)} \geqslant \ldots \geqslant x_{\pi(n)} \geqslant 0 \right\}. \tag{13}$$

The collection of simplices $\{ \mathbf{T}_\pi \}_{\pi \in \mathcal{S}_n}$, whose union is $[0,1]^n$, is known as the *Kuhn triangulation* of $[0,1]^n$ [42].

The number of simplices in the Kuhn triangulation is exponential, so an n-dimensional generalization of Example 1 could contain an exponential number of inequalities in (12c). Fortunately, as illustrated in the following example, the characterization of $\mathbf{T}_\pi$ in the right hand side of (13) allow us to easily filter for relevant inequalities.

Example 1 continued. *Consider the point $(x^*, y^*) = (0.6, 0.3, 0.5)$ depicted as a red star in Figure 3c. To check if $(x^*, y^*) \in \mathrm{Conv}(S)$ we can first verify that $y^* \geqslant g(x^*)$ and $x^* \in [0,1]^2$. It then only remains to check that (x^*, y^*) satisfies all inequalities in* (12c)*. However, we can instead exploit the fact that if $x \in \mathbf{T}_1$, then $r_1(x) = \min\{ r_1(x), r_2(x) \}$. As illustrated in Figure 3c we can use the fact that $x_1^* \geqslant x_2^*$ to conclude that x^* (depicted as a red circle in Figure 3c) belongs to $\mathbf{T}_1$. Finally, we can check that $r_1(x^*) = 0.3 < 0.5$ to conclude that $(x^*, y^*) \notin \mathrm{Conv}(S)$ (Point $(x^*, 0.3)$ is depicted as a red diamond in Figure 3c).*

To show that the ideas in Example 1 can be generalized, we will exploit properties of submodular functions. For that we connect functions from $[0,1]^n$ with set-functions. We pick one specific connection that simplifies the statement and proof of Theorem 1.

Definition 2. *A set-function $H : 2^{[\![n]\!]} \to \mathbb{R}$ is submodular if*

$$H(S) + H(T) \geqslant H(S \cup T) + H(S \cap T) \quad \forall S, T \subseteq [\![n]\!] .$$

For any $h : [0,1]^n \to \mathbb{R}$ we define the set-function $H : 2^{[\![n]\!]} \to \mathbb{R}$ given by $H(I) = h\left(\sum_{i \notin I} e(i)\right)$ for each $I \subseteq [\![n]\!]$. In particular, $H([\![n]\!]) = h(\mathbf{0}^n)$ and $H(\varnothing) = h(\mathbf{1}^n)$. In general, for any function from $[0,1]^n$ to $\mathbb{R}$ defined as a lower case letter (e.g. h), we let the associated set-function be defined by the upper case version of this letter (e.g. H).

A.1.2 Proof of Theorem 1

Our proof has three steps. First, we formalize the idea in Example 1 for arbitrary dimensions (Theorem 2). Then, we reduce the number of inequalities by characterizing which of the simplices $\mathbf{T}_\pi$ lead to identical inequalities (Lemma 2). Finally, to complete the proof of Theorem 1, we describe the explicit form of these inequalities.

Corollary 3.14 in [40] gives us a precise description of $\mathrm{Conv}(Q)$ where Q is a normalized version of S from (5) that also considers any convex activation function. We include a submodularity-based proof of the corollary for completeness, adapted to our context.

Theorem 2. *Let $w \in \mathbb{R}^n_+$ and $b \in \mathbb{R}$, $f(x) = w \cdot x + b$, $\rho : \mathbb{R} \to \mathbb{R}$ be any convex function, $g(x) = \rho(f(x))$ and $Q = \{\, (x,y) \in [0,1]^n \times \mathbb{R} \mid y = \rho(f(x)) \,\}$.*

For each $\pi \in \mathcal{S}_n$ let $r_\pi : [0,1]^n \to \mathbb{R}$ be the unique affine interpolation[9] of g on $\mathbf{T}_\pi$ such that $r_\pi(v) = g(v)$ for all $v \in \mathbf{V}_\pi$. Then $\mathrm{Conv}(Q)$ equals the set of all $(x,y) \in \mathbb{R}^n \times \mathbb{R}$ satisfying

$$y \geqslant g(x) \tag{14a}$$

$$y \leqslant r_\pi(x) \qquad \forall \pi \in \mathcal{S}_n \tag{14b}$$

$$0 \leqslant x_i \leqslant 1 \qquad \forall i \in [\![n]\!] \tag{14c}$$

Proof. Let $h : [0,1]^n \to \mathbb{R}$ be such that $h(x) = -g(x) = -\rho(f(x))$ for all $x \in [0,1]^n$. In addition, let $\underline{h}$ and $\overline{h}$ respectively be the convex and concave envelopes of h (i.e. the largest convex underestimator of h, which is well-defined because the pointwise maximum of convex functions lying below h is a convex function, and the smallest concave overestimator of h, which is similarly well-defined). Then $Q = \{\, (x,y) \in [0,1]^n \times \mathbb{R} \mid -y = h(x) \,\}$ and $\mathrm{Conv}(Q) = \left\{\, (x,y) \in [0,1]^n \times \mathbb{R} \;\middle|\; \underline{h}(x) \leqslant -y \leqslant \overline{h}(x) \,\right\}$ (e.g. [32, Proposition B.1]). Function h is concave and hence $\overline{h} = h$, so it only remains to describe $\underline{h}$.

To describe $\underline{h}$, we define a set function H based on h (see Definition 2), which is submodular because $-\rho$ is concave and w is non-negative (e.g. see [1, Section 3.1]). Submodularity allows us to describe the lower convex envelope of the continuous function h through the *Lovász extension* of the set function H. This extension is the piecewise affine function from $[0,1]^n$ to $\mathbb{R}$ defined over the pieces $\{\mathbf{T}_\pi : \pi \in \mathcal{S}_n\}$, which equals $\max_{\pi \in \mathcal{S}_n}(-r_\pi)$ by convexity (e.g. see [6] for further details). Therefore the constraint required for $\mathrm{conv}(Q)$ is $\underline{h}(x) \leqslant -y \iff y \leqslant \min_{\pi \in \mathcal{S}_n} r_\pi(x)$ which completes the derivation of inequalities (14b) in the theorem statement. $\square$

Note that even though there are exponentially many inequalities in (14b), the tightest constraint on y at any given point $x \in [0,1]^n$ can be efficiently found, by sorting the coordinates of x to find the simplex $\mathbf{T}_\pi$ to which x belongs. Moreover, going from $[0,1]^n$ to $[L, U]$ and eliminating the sign restriction on w can be achieved with standard variable transformations (e.g. see the comments before [40, Corollary 3.14]).

Before demonstrating the variable transformations, we first further refine Theorem 2 for the case when ρ is equal to the ReLU activation function σ. In particular, we generally have that each one of the $n!$ inequalities in (14b) is facet-defining because they hold at equality over the $n+1$ affinely independent points $\{\, (v, g(v)) \,\}_{v \in \mathbf{V}_\pi}$. Hence, they are all needed to describe $\mathrm{Conv}(R)$. However, because it may happen that $r_\pi = r_{\pi'}$ for $\pi \neq \pi'$, the number of inequalities in (14b) after removing duplicates may be much smaller. The following lemma shows that this is indeed the case when ρ is equal to the ReLU activation function σ. The lemma also gives a closed form expression for the interpolating functions r_π in this case.

[9] Such an affine interpolation exists and is unique because $\mathbf{V}_\pi$ is a set of $n+1$ affinely independent points.

Lemma 2. *Let $w \in \mathbb{R}^n_+$ and $-\sum_{i=1}^n w_i \leqslant b < 0$, $f(x) = w \cdot x + b$, and $g(x) = \sigma(f(x))$. If $\{ r_\pi \}_{\pi \in \mathcal{S}_n}$ are the affine interpolation functions from Theorem 2, then*

$$\left\{ (x, y) \in \mathbb{R}^{n+1} \,\middle|\, y \leqslant r_\pi(x) \quad \forall \pi \in \mathcal{S}_n \right\} = \left\{ (x, y) \in \mathbb{R}^{n+1} \,\middle|\, y \leqslant r_{I,h}(x) \quad \forall (I, h) \in \mathcal{I} \right\}$$

where $\mathcal{I} \overset{\text{def}}{=} \left\{ (I, h) \in 2^{[\![n]\!]} \times [\![n]\!] \,\middle|\, F(I) \geqslant 0,\ F(I \cup \{h\}) < 0 \right\}$, $r_{I,h}(x) \overset{\text{def}}{=} F(I)x_h + \sum_{i \in I} w_i x_i$, and $F : 2^{[\![n]\!]} \to \mathbb{R}$ is the set-function associated to f as defined in Definition 2.

Proof. Fix $\pi \in \mathcal{S}_n$ and for each $j \in [\![n]\!]$ let $I(j) \overset{\text{def}}{=} \{ \pi(i) \}_{i=j+1}^n$.

Then the interpolation condition for r_π given by $r_\pi(v) = g(v)$ for all $v \in \mathbf{V}_\pi$ is equivalent to

$$R_\pi(I(j)) = G(I(j)) \quad \forall j = 0, 1, \ldots, n \tag{15}$$

where R_π and G are the set-functions associated to r_π and g as defined in Definition 2. For $j = 0$, condition (15) implies $r_\pi(\mathbf{0}^n) = R_\pi([\![n]\!]) = G([\![n]\!]) = g(\mathbf{0}^n) = 0$ and hence there exists $\alpha \in \mathbb{R}^n$ such that $r_\pi(x) = \alpha \cdot x$ (i.e. r_π is a linear function). For $j \in [\![n]\!]$, condition (15) further implies that

$$\alpha_{\pi(j)} = g\left(\sum_{i=0}^{j} e(\pi(i))\right) - g\left(\sum_{i=0}^{j-1} e(\pi(i))\right) = G(I(j)) - G(I(j-1)) \quad \forall j \in [\![n]\!]. \tag{16}$$

Now, because $F(\varnothing) = f(\mathbf{1}^n) \geqslant 0$, $w \in \mathbb{R}^n_+$, and $b < 0$, there exists a unique $k \in [\![n]\!]$ such that $(I(k), \pi(k)) \in \mathcal{I}$. Furthermore, $w \in \mathbb{R}^n_+$, $F(I(k) \cup \{ \pi(k) \}) = F(I(k-1)) < 0$, and $F(I(k)) \geqslant 0$ imply

$$F(I(j)) < 0 \quad \text{and} \quad G(I(j)) = 0 \qquad \forall j = 0, \ldots, k-1; \tag{17a}$$

$$F(I(j)) \geqslant 0 \quad \text{and} \quad G(I(j)) = F(I(j)) \quad \forall j = k, \ldots, n. \tag{17b}$$

Equations (16) and (17a) imply $\alpha_{\pi(j)} = 0$ for all $j \in [\![k]\!]$ or equivalently $\alpha_i = 0$ for all $i \notin I(k) \cup \{ \pi(k) \}$. Equations (16) and (17) imply $\alpha_{\pi(k)} = G(I(k)) = F(I(k))$. Finally, equations (16) and (17b) imply that $\alpha_{\pi(j)} = w_{\pi(j)}$ for all $j = k+1, \ldots, n$ or equivalently $\alpha_i = w_i$ for all $i \in I$. Hence, $r_\pi = r_{I(k), \pi(k)}$. The lemma follows by noting that for any $(I, h) \in \mathcal{I}$ there exists at least one $\pi \in \mathcal{S}_n$ such that $(I(k), \pi(k)) = (I, h)$. □

Finally, we obtain the proof of Theorem 1 recalling that $f(x) = w \cdot x + b$ for $w \in \mathbb{R}^n$ and $b \in \mathbb{R}$, and $S = \{ (x, y) \in [L, U] \times \mathbb{R} \mid y = \sigma(f(x)) \}$ for $L, U \in \mathbb{R}^n$ such that $L < U$.

Theorem 1. *If $\ell([\![n]\!]) \geqslant 0$, then* $\operatorname{Conv}(S) = S = \{ (x, y) \in [L, U] \times \mathbb{R} \mid y = f(x) \}$. *Alternatively, if $\ell(\varnothing) < 0$, then* $\operatorname{Conv}(S) = S = [L, U] \times \{ 0 \}$. *Otherwise,* $\operatorname{Conv}(S)$ *is equal to the set of all $(x, y) \in \mathbb{R}^n \times \mathbb{R}$ satisfying*

$$y \geqslant w \cdot x + b, \quad y \geqslant 0, \quad L \leqslant x \leqslant U \tag{6a}$$

$$y \leqslant \sum_{i \in I} w_i (x_i - \breve{L}_i) + \frac{\ell(I)}{\breve{U}_h - \breve{L}_h}(x_h - \breve{L}_h) \qquad \forall (I, h) \in \mathcal{J}. \tag{6b}$$

Furthermore, if $d \overset{\text{def}}{=} |\{ i \in [\![n]\!] \mid w_i \neq 0 \}|$, then $d \leqslant |\mathcal{J}| \leqslant \lceil \frac{1}{2} d \rceil \binom{d}{\lceil \frac{1}{2} d \rceil}$ and for each of these inequalities (and each $d \in [\![n]\!]$) there exist data that makes it hold at equality.

Proof. Recalling that $\mathcal{J} \overset{\text{def}}{=} \left\{ (I, h) \in 2^{[\![n]\!]} \times [\![n]\!] \,\middle|\, \ell(I) \geqslant 0, \quad \ell(I \cup \{h\}) < 0, \quad w_i \neq 0 \quad \forall i \in I \right\}$ we can assume without loss of generality that $w_i \neq 0$ for all $i \in [\![n]\!]$ and hence $d = n$ (Indices i with $w_i = 0$ do not affect (6b) or the definition of $\mathcal{J}$ and the only inequalities for S or $\operatorname{Conv}(S)$ in which a given x_i appears are $L_i \leqslant x_i \leqslant U_i$).

For the first case, the result follows because $f(x) < 0$ for all $x \in [L, U]$ and hence $g(x) = 0$ for all $x \in [L, U]$.

For the second case, the result follows because $f(x) \geqslant 0$ for all $x \in [L, U]$ and hence $g(x) = f(x)$ for all $x \in [L, U]$.

For the third case, recall that $\breve{L}_i = \begin{cases} L_i & w_i \geqslant 0 \\ U_i & \text{o.w.} \end{cases}$ and $\breve{U}_i = \begin{cases} U_i & w_i \geqslant 0 \\ L_i & \text{o.w.} \end{cases}$, and consider the affine variable transformation given by

$$\breve{x}_i \overset{\text{def}}{=} \frac{x_i - \breve{L}_i}{\breve{U}_i - \breve{L}_i} \quad \text{and} \quad x_i = (\breve{U}_i - \breve{L}_i)\breve{x}_i + \breve{L}_i \quad \forall i \in [\![n]\!]. \tag{18}$$

Let $\breve{w}_i \overset{\text{def}}{=} w_i(\breve{U}_i - \breve{L}_i)$ for each $i \in [\![n]\!]$, $\breve{b} \overset{\text{def}}{=} b + \sum_{i=1}^n w_i \breve{L}_i = \ell([\![n]\!]) < 0$, and $\breve{f}(\breve{x}) \overset{\text{def}}{=} \breve{w} \cdot \breve{x} + \breve{b}$ (recall that $\ell(I) \overset{\text{def}}{=} \sum_{i \in I} w_i \breve{L}_i + \sum_{i \notin I} w_i \breve{U}_i + b$). Then we may infer that

$$\breve{w}_i \breve{x}_i = w_i(x_i - \breve{L}_i) \quad \forall i \in [\![n]\!], \tag{19}$$

that $f(x) = \breve{f}(\breve{x})$, and finally that $(x, y) \in S$ if and only if $(\breve{x}, y) \in \breve{S} \overset{\text{def}}{=} \left\{ (\breve{x}, y) \in [0,1]^n \times \mathbb{R} \;\middle|\; y = \sigma(\breve{f}(\breve{x})) \right\}$.

In addition, we conclude $\breve{w} \in \mathbb{R}^n_+$, using the definition of $\breve{L}$ and $\breve{U}$ and the fact that $L < U$. Hence, Theorem 2 and Lemma 2 are applicable for $\breve{S}$ and $\breve{g}(\breve{x}) = \sigma(\breve{f}(\breve{x}))$. Then

$$\operatorname{Conv}(\breve{S}) = \left\{ (\breve{x}, y) \in [0,1]^n \times \mathbb{R}_+ \;\middle|\; \breve{f}(\breve{x}) \leqslant y \leqslant r_{I,h}(\breve{x}) \quad \forall (I, h) \in \mathcal{I} \right\}$$

where $\mathcal{I} = \left\{ (I, h) \in 2^{[\![n]\!]} \times [\![n]\!] \;\middle|\; \breve{F}(I) \geqslant 0,\ \breve{F}(I \cup \{h\}) < 0 \right\}$ and $r_{I,h}(\breve{x}) = \breve{F}(I)\breve{x}_h + \sum_{i \in I} \breve{w}_i \breve{x}_i$. Using the definitions of $\breve{b}$ and $\breve{w}_i$ we get

$$\breve{F}(I) = \sum_{i \notin I} \breve{w}_i + \breve{b} = \sum_{i \notin I} w_i \left(\breve{U}_i - \breve{L}_i \right) + \left(b + \sum_{i=1}^n w_i \breve{L}_i \right) = \sum_{i \notin I} w_i \breve{U}_i + \sum_{i \in I} w_i \breve{L}_i + b = \ell(I) \tag{20}$$

and hence $\mathcal{I} = \mathcal{J} = \left\{ (I, h) \in 2^{[\![n]\!]} \times [\![n]\!] \mid \ell(I) \geqslant 0,\ \ell(I \cup \{h\}) < 0 \right\}$. Combining (18–20), we get

$$\breve{r}_{I,h}(\breve{x}) = \breve{F}(I)\breve{x}_h + \sum_{i \in I} \breve{w}_i \breve{x}_i = \ell(I) \frac{x_h - \breve{L}_h}{\breve{U}_h - \breve{L}_h} + \sum_{i \in I} w_i \left(x_i - \breve{L}_i \right).$$

Hence, $\operatorname{Conv}(S)$ is described by (6).

Finally, $(I, h) \in \mathcal{J}$ if and only if the hyperplane $\sum_{i=1}^n w_i x_i + b = 0$ cuts the edge uv of $[0,1]^n$ given by $u \overset{\text{def}}{=} \sum_{i \notin (I \cup \{h\})} e(i)$ and $v \overset{\text{def}}{=} \sum_{i \notin I} e(i)$ (with the convention that an empty sum is equal to zero). The result on $|\mathcal{J}|$ then follows by Lemma 1 recalling that without loss of generality we have assumed $n = d$.

□

A.2 An alternative proof using mixed-integer programming and projection

We can alternatively prove Theorem 1 by connecting it to the MIP formulation from [3] for S defined in (5). For this, first recall that that $f(x) = w \cdot x + b$ for $w \in \mathbb{R}^n$ and $b \in \mathbb{R}$, and $S = \{ (x, y) \in [L, U] \times \mathbb{R} \mid y = \sigma(f(x)) \}$ for $L, U \in \mathbb{R}^n$ such that $L < U$.

Corollary 2. *Let*

$$R_{\text{sharp}} \overset{\text{def}}{=} \left\{ (x, y, z) \in [L, U] \times \mathbb{R} \times [0,1]^2 \;\middle|\; \begin{array}{c} y \geqslant 0, \\ y \geqslant w \cdot x + b, \\ y \leqslant \bar{f}(x, z), \\ z_1 + z_2 = 1 \end{array} \right\},$$

where

$$\bar{f}(x, z) \overset{\text{def}}{=} \max_{\tilde{x}^1, \tilde{x}^2} \left\{ w \cdot \tilde{x}^2 + b z_2 \;\middle|\; \begin{array}{cc} x = \tilde{x}^1 + \tilde{x}^2, & \\ L z_k \leqslant \tilde{x}^k \leqslant U z_k & \forall k \in [\![2]\!] \\ \tilde{x}^1, \tilde{x}^2 \in \mathbb{R}^n & \end{array} \right\}.$$

Then $\operatorname{Conv}(S) = \operatorname{Proj}_{x,y}(R_{\text{sharp}}) \overset{\text{def}}{=} \left\{ (x, y) \in \mathbb{R}^{n+1} \;\middle|\; \exists z \in \mathbb{R}^2 \ \textit{s.t.} \ (x, y, x) \in R_{\text{sharp}} \right\}$.

Proof. Follows from [3, Proposition 5] for the case $d = 2$, $w^1 = 0$, $b^1 = 0$, $w^2 = w$, $b^2 = b$. □

Lemma 3. *Let*

$$R \overset{\text{def}}{=} \left\{ (x,y) \in [L,U] \times \mathbb{R} \;\middle|\; \begin{array}{l} y \geqslant 0, \\ y \geqslant w \cdot x + b, \\ y \leqslant \tilde{f}(x) \end{array} \right\}$$

where

$$\tilde{f}(x) \overset{\text{def}}{=} \max_{\tilde{x}^1, \tilde{x}^2, z} \left\{ w \cdot \tilde{x}^2 + b z_2 \;\middle|\; \begin{array}{ll} x = \tilde{x}^1 + \tilde{x}^2, & \\ L z_k \leqslant \tilde{x}^k \leqslant U z_k & \forall k \in [\![2]\!] \\ \tilde{x}^1, \tilde{x}^2 \in \mathbb{R}^n & \\ z_1 + z_2 = 1 & \\ z \in [0,1]^2 & \end{array} \right\}. \tag{21}$$

Then $\operatorname{Conv}(S) = R$.

Proof. By Corollary 2 it suffices to show $R = \operatorname{Proj}_{x,y}(R_{\text{sharp}})$.

Inclusion $\operatorname{Proj}_{x,y}(R_{\text{sharp}}) \subseteq R$ follows by noting that $\bar{f}(\hat{x}, \hat{z}) \leqslant \tilde{f}(\hat{x})$ for any $(\hat{x}, \hat{y}, \hat{z}) \in R_{\text{sharp}}$.

For inclusion $R \subseteq \operatorname{Proj}_{x,y}(R_{\text{sharp}})$, let $(\hat{x}, \hat{y}) \in R$, and let $\left(\tilde{x}^1, \tilde{x}^2, z\right) \in \mathbb{R}^{2n+2}$ be an optimal solution to the optimization problem in the right hand side of (21) for $x = \hat{x}$. Such solution exists because for $\hat{x} \in [L,U]$ this optimization problem is the maximization of a linear function over a non-empty bounded polyhedron. Then, $\tilde{f}(\hat{x}) = \bar{f}(\hat{x}, z)$, and hence $(\hat{x}, \hat{y}, z) \in R_{\text{sharp}}$. ☐

Theorem 1. *If* $\ell([\![n]\!]) \geqslant 0$*, then* $\operatorname{Conv}(S) = S = \{\, (x,y) \in [L,U] \times \mathbb{R} \mid y = f(x) \,\}$*. Alternatively, if* $\ell(\varnothing) < 0$*, then* $\operatorname{Conv}(S) = S = [L,U] \times \{\, 0 \,\}$*. Otherwise,* $\operatorname{Conv}(S)$ *is equal to the set of all* $(x,y) \in \mathbb{R}^n \times \mathbb{R}$ *satisfying*

$$y \geqslant w \cdot x + b, \quad y \geqslant 0, \quad L \leqslant x \leqslant U \tag{6a}$$

$$y \leqslant \sum\nolimits_{i \in I} w_i (x_i - \breve{L}_i) + \frac{\ell(I)}{\breve{U}_h - \breve{L}_h}(x_h - \breve{L}_h) \qquad \forall (I,h) \in \mathcal{J}. \tag{6b}$$

Furthermore, if $d \overset{\text{def}}{=} |\{\, i \in [\![n]\!] \mid w_i \neq 0 \,\}|$*, then* $d \leqslant |\mathcal{J}| \leqslant \lceil \frac{1}{2} d \rceil \binom{d}{\lceil \frac{1}{2} d \rceil}$ *and for each of these inequalities (and each* $d \in [\![n]\!]$*) there exist data that makes it hold at equality.*

Proof. Recalling that $\mathcal{J} \overset{\text{def}}{=} \left\{\, (I,h) \in 2^{[\![n]\!]} \times [\![n]\!] \;\middle|\; \ell(I) \geqslant 0, \quad \ell(I \cup \{h\}) < 0, \quad w_i \neq 0 \quad \forall i \in I \,\right\}$ we can assume without loss of generality that $w_i \neq 0$ for all $i \in [\![n]\!]$ and hence $d = n$ (Indices i with $w_i = 0$ do not affect (6b) or the definition of $\mathcal{J}$ and the only inequalities for S or $\operatorname{Conv}(S)$ in which x_i appear for such index are $L_i \leqslant x_i \leqslant U_i$).

For the first case, the result follows because $f(x) < 0$ for all $x \in [L,U]$ and hence $g(x) = 0$ for all $x \in [L,U]$.

For the second case, the result follows because $f(x) \geqslant 0$ for all $x \in [L,U]$ and hence $g(x) = f(x)$ for all $x \in [L,U]$.

For the third case, it suffices to show that

$$\tilde{f}(x) = \min_{(I,h) \in \mathcal{J}} \left\{ \sum_{i \in I} w_i (x_i - \breve{L}_i) + \frac{\ell(I)}{\breve{U}_h - \breve{L}_h}(x_h - \breve{L}_h) \right\}, \tag{22}$$

in which case, set R from Lemma 3 is exactly the set described by (6). To show (22) we first simplify the optimization problem defining $\tilde{f}(x)$ by applying the simple substitutions $\tilde{x} \overset{\text{def}}{=} \tilde{x}^2 = x - \tilde{x}^1$ and $z \overset{\text{def}}{=} z_2 = 1 - z_1$:

$$\tilde{f}(x) = \max_{\tilde{x}, z} \left\{ w \cdot \tilde{x} + bz \;\middle|\; \begin{array}{rl} L(1-z) \leqslant x - \tilde{x} & \leqslant U(1-z), \\ Lz \leqslant \quad \tilde{x} & \leqslant Uz, \\ z \in & [0,1] \end{array} \right\}.$$

This optimization problem is feasible and bounded when $L \leqslant x \leqslant U$, and thus we may assume an optimal solution exists.

Consider some $i \in [\![n]\!]$. If $w_i > 0$, then $\tilde{x}_i \geqslant L_i z$ and $x_i - \tilde{x}_i \leqslant U_i(1-z)$ hold at any optimal solution, since we are maximizing the problem and each constraint involves only a single x_i and z. Analogously, if $w_i < 0$, then $\tilde{x}_i \leqslant U_i z$ and $x_i - \tilde{x}_i \geqslant L_i(1-z)$ are implied as well. To unify these two cases into one as a simplification, observe that these constraints can be expressed as $w_i\tilde{x}_i \geqslant w_i\breve{L}_i z$ and $w_i(x_i - \tilde{x}_i) \leqslant w_i\breve{U}_i(1-z)$ respectively (recall that $w_i \neq 0$ by assumption, and that $\breve{L}_i = L_i$ if $w_i \geqslant 0$, or U_i otherwise, and $\breve{U}_i = U_i$ if $w_i \geqslant 0$, or L_i otherwise). Therefore, we can drop these constraints and keep the remaining ones:

$$\tilde{f}(x) = \max_{\tilde{x},z} \left\{ w \cdot \tilde{x} + bz \;\middle|\; \begin{array}{ll} w_i(x_i - \tilde{x}_i) \geqslant w_i\breve{L}_i(1-z) & \forall i \in [\![n]\!], \\ w_i\tilde{x}_i \leqslant w_i\breve{U}_i z & \forall i \in [\![n]\!] \\ z \in [0,1] & \end{array} \right\}.$$

Define $\gamma_i \overset{\text{def}}{=} w_i(\breve{U}_i z - \tilde{x}_i)$ for all $i \in [\![n]\!]$. We can then rewrite the problem as:

$$\tilde{f}(x) = \max_{\gamma,z} \left\{ (w \cdot \breve{U} + b)z - \sum_{i=1}^{n} \gamma_i \;\middle|\; \begin{array}{ll} w_i(\breve{U}_i - \breve{L}_i)z - \gamma_i \leqslant w_i(x_i - \breve{L}_i) & \forall i \in [\![n]\!] \\ \gamma \geqslant 0, & \\ z \in [0,1] & \end{array} \right\}.$$

We next take the dual of this problem. By strong duality, the following holds:

$$\tilde{f}(x) = \min_{\alpha,\beta} \left\{ \sum_{i=1}^{n} w_i(x_i - \breve{L}_i)\alpha_i + \beta \;\middle|\; \begin{array}{c} \sum_{i=1}^{n} w_i(\breve{U}_i - \breve{L}_i)\alpha_i + \beta \geqslant \sum_{i=1}^{n} w_i\breve{U}_i + b, \\ \alpha \in [0,1]^n, \\ \beta \geqslant 0 \end{array} \right\}.$$

To conclude the proof, we describe the optimal solutions of the optimization problem above. Note that it is a minimization variant of a fractional knapsack problem and it can be solved by a greedy algorithm, in which we order the indices of α by $\frac{x_i - \breve{L}_i}{\breve{U}_i - \breve{L}_i}$ and maximally select those with the smallest ratios, until the knapsack constraint is satisfied at equality. We also need to consider β in the knapsack, but since the ratios for α_i are in $[0,1]$ and the ratio for β is 1, β would only be picked last. Moreover, under the assumptions of our current third case, we have $\ell([\![n]\!]) = \sum_{i=1}^{n} w_i\breve{L}_i + b < 0$, and thus that we can satisfy the knapsack constraint by choosing from α's (recall that $\ell(I) = \sum_{i\in I} w_i\breve{L}_i + \sum_{i\notin I} w_i\breve{U}_i + b$). Therefore we may set $\beta = 0$.

Let I be the set of indices in which $\alpha_i = 1$ for the optimal solution and h be the next index to be considered by the greedy procedure after the elements in I. Then

$$\alpha_h = \frac{\left(\sum_{i=1}^{n} w_i\breve{U}_i + b\right) - \left(\sum_{i\in I} w_i(\breve{U}_i - \breve{L}_i)\right)}{\breve{U}_h - \breve{L}_h} = \frac{\ell(I)}{\breve{U}_h - \breve{L}_h} \in [0,1).$$

Observe that $\ell(I) \geqslant 0$ is equivalent to stating that the items in I are below the knapsack capacity, since $\ell(I)$ equals the capacity of the knapsack minus the total weight of the items in I. Therefore, $\ell(I) \geqslant 0$ and $\ell(I \cup \{h\}) < 0$ (i.e. the items in I fit but we can only add h partially). Hence, we can write the optimization problem defining $\tilde{f}(x)$ as finding the optimal I and h:

$$\tilde{f}(x) = \min_{I,h\notin I} \left\{ \sum_{i\in I} w_i(x_i - \breve{L}_i) + \frac{\ell(I)}{\breve{U}_h - \breve{L}_h}(x_h - \breve{L}_h) \mid \ell(I) \geqslant 0,\ \ell(I \cup \{h\}) < 0 \right\}.$$

We obtain (22) by recalling that $\mathcal{J} = \left\{ (I,h) \in 2^{[\![n]\!]} \times [\![n]\!] \;\middle|\; \ell(I) \geqslant 0,\ \ell(I \cup \{h\}) < 0 \right\}$.

Finally, $(I,h) \in \mathcal{J}$ if and only if the hyperplane $\sum_{i=1}^{n} w_i x_i + b = 0$ cuts the edge uv of $[0,1]^n$ given by $u \overset{\text{def}}{=} \sum_{i\notin(I\cup\{h\})} e(i)$ and $v \overset{\text{def}}{=} \sum_{i\notin I} e(i)$ (with the convention that an empty sum is equal to zero). The result on $|\mathcal{J}|$ then follows by Lemma 1 recalling that without loss of generality we have assumed $n = d$. □

B Proofs of other results from Section 3

Proposition 1. *For any input dimension n, there exists a point $\tilde{x} \in \mathbb{R}^n$, and a problem instance given by the affine function f, the Δ-relaxation C_Δ, and the single neuron set S such that* $\left(\max_{y:(f(\tilde{x}),y)\in C_\Delta} y\right) - \left(\max_{y:(\tilde{x},y)\in \mathrm{Conv}(S)} y\right) = \Omega(n)$.

Proof. This follows as a straightforward extension of [3, Example 2], as the Δ-relaxation is equal to the projection of the big-M formulation presented in that work. □

The following proposition shows how the additional structure in Lemma 2 allows increasing the speed of checking for violated inequalities from $\mathcal{O}(n\log(n))$, achievable by sorting the input components, to $\mathcal{O}(n)$.

Proposition 2. *The optimization problem* (7) *can be solved in* $\mathcal{O}(n)$ *time.*

Proof. Recall that $\mathcal{J} \overset{\text{def}}{=} \left\{ (I,h) \in 2^{[\![n]\!]} \times [\![n]\!] \;\middle|\; \ell(I) \geqslant 0, \quad \ell(I \cup \{h\}) < 0, \quad w_i \neq 0\ \forall i \in I \right\}$, $\ell(I) \overset{\text{def}}{=} \sum_{i\in I} w_i \breve{L}_i + \sum_{i\notin I} w_i \breve{U}_i + b$, $\breve{L}_i \overset{\text{def}}{=} \begin{cases} L_i & w_i \geqslant 0 \\ U_i & \text{o.w.}\end{cases}$ and $\breve{U}_i \overset{\text{def}}{=} \begin{cases} U_i & w_i \geqslant 0 \\ L_i & \text{o.w.}\end{cases}$ for each $i \in [\![n]\!]$, and (7) is the optimization problem given by

$$v(x) \overset{\text{def}}{=} \min\left\{ \sum\nolimits_{i\in I} w_i(x_i - \breve{L}_i) + \frac{\ell(I)}{\breve{U}_h - \breve{L}_h}(x_h - \breve{L}_h) \;\middle|\; (I,h) \in \mathcal{J} \right\}.$$

First, we can check in $\mathcal{O}(n)$ time if $\ell([\![n]\!]) \geqslant 0$ or $\ell(\varnothing) < 0$, in which case $\mathcal{J} = \varnothing$ and (7) is infeasible. Otherwise, $\ell([\![n]\!]) < 0$, $\ell(\varnothing) \geqslant 0$, and $\mathcal{J} \neq \varnothing$.

We can also remove in $\mathcal{O}(n)$ time all $i \in [\![n]\!]$ such that $w_i = 0$. Then without loss of generality we may assume that $w_i \neq 0$ for all $i \in [\![n]\!]$ and hence $L < U$ implies that

$$w_i(\breve{U}_i - \breve{L}_i) > 0 \quad \forall i \in [\![n]\!]. \tag{23}$$

We will show that (7) is equivalent to the linear programming problem

$$\begin{aligned} \omega(x) \overset{\text{def}}{=} \min_v \quad & \sum_{i=1}^n w_i(x_i - \breve{L}_i)v_i && \text{(24a)}\\ \text{s.t.} \quad & \sum_{i=1}^n w_i(\breve{U}_i - \breve{L}_i)v_i = \sum_{i=1}^n w_i\breve{U}_i + b, && \text{(24b)}\\ & 0 \leqslant v \leqslant 1. && \text{(24c)} \end{aligned}$$

Note that the set of basic feasible solutions for the linear programming problem is exactly the set of all feasible points with at most one fractional component (see, e.g., [7, Chapter 3]). That is, all basic feasible solutions of (24) are elements of $\mathcal{V} \overset{\text{def}}{=} \{ v \in [0,1]^n \mid |\{ i \in [\![n]\!] \mid v_i \in (0,1) \}| \leqslant 1 \}$.

To prove that $\omega(x) \leqslant v(x)$, consider the mapping $\Phi : \mathcal{J} \to \mathcal{V}$ given by

$$\Phi\left((I,h)\right)_i = \begin{cases} 1 & i \in I \\ \frac{\ell(I)}{w_h(\breve{U}_h - \breve{L}_h)} & i = h \\ 0 & \text{o.w.} \end{cases} \quad \forall i \in [\![n]\!].$$

Let $(\bar{I},\bar{h}) \in \mathcal{J}$ be an optimal solution for (7) and let $\bar{v} = \Phi\left((\bar{I},\bar{h})\right)$. Then

$$\sum_{i=1}^n w_i(\breve{U}_i - \breve{L}_i)\bar{v}_i = \sum_{i\in\bar{I}} w_i(\breve{U}_i - \breve{L}_i) + w_{\bar{h}}(\breve{U}_{\bar{h}} - \breve{L}_{\bar{h}})\frac{\ell(\bar{I})}{w_{\bar{h}}(\breve{U}_{\bar{h}} - \breve{L}_{\bar{h}})} = \sum_{i=1}^n w_i\breve{U}_i + b,$$

and hence $\bar{v}$ satisfies (24b). Algebraic manipulation shows that

$$w_h(\breve{U}_h - \breve{L}_h) = \ell(I) - \ell(I \cup \{h\}) \quad \forall I \subseteq [\![n]\!], \quad h \in [\![n]\!]\backslash I. \tag{25}$$

In addition, $(\bar{I}, \bar{h}) \in \mathcal{J}$ implies $\ell(\bar{I}) \geqslant 0$ and $\ell(\bar{I} \cup \{\bar{h}\}) < 0$. Combining this with (25) gives the inequality $\ell(\bar{I}) < w_{\bar{h}}(\breve{U}_{\bar{h}} - \breve{L}_{\bar{h}})$. Therefore, $\bar{v}_h \in [0,1)$, and hence $\bar{v}_h$ is feasible for (24). In addition, for any $(I, h) \in \mathcal{J}$ we have that

$$\sum_{i=1}^{n} w_i(x_i - \breve{L}_i)\bar{v}_i = \sum_{i \in I} w_i(x_i - \breve{L}_i) + w_h(\breve{U}_h - \breve{L}_h)\frac{\ell(I)}{w_h(x_h - \breve{L}_h)}$$

and hence the objective value of $\bar{v}_h$ for (24) is the same as the objective value of (I, h) for (7).

To prove $\omega(x) \geqslant v(x)$ we will show that, through Φ, the greedy procedure to solve (7) described in the main text just before the statement of Proposition 2, becomes the standard greedy procedure for (24) and hence also yields an optimal basic feasible solution to (24). For simplicity, assume without loss of generality that we have re-ordered the indices in $[\![n]\!]$ so that

$$\frac{x_1 - \breve{L}_1}{\breve{U}_1 - \breve{L}_1} \leqslant \frac{x_2 - \breve{L}_2}{\breve{U}_2 - \breve{L}_2} \leqslant \cdots \leqslant \frac{x_n - \breve{L}_n}{\breve{U}_n - \breve{L}_n}. \tag{26}$$

Then the greedy procedure that incrementally grows I terminates with some $(I, h) \in \mathcal{J}$ where $I = [\![h-1]\!]$. Then $v = \Phi\left(([\![h-1]\!], h)\right)$ is a basic feasible solution for (24) with the same objective value as the objective value of (I, h) for (7). To conclude that $\omega(x) \geqslant v(x)$, we claim that v is an optimal solution for (24) since the standard greedy procedure for (24) is known to generate the optimal solution for this problem. For completeness, we give the following self contained proof of the claim. Assume for a contradiction that $\omega(x) < \sum_{i=1}^{n} w_i(x_i - \breve{L}_i)v_i$ and let v' be an optimal solution to (24). Because $v' \neq v$ and both v and v' satisfy (24b), (23) implies there must exists $j_1, j_2 \in [\![n]\!]$ such that $j_1 < j_2$, $j_1 \leqslant h$, $v'_{j_1} < v_{j_1}$, $j_2 \geqslant h$ and $v'_{j_2} > v_{j_2}$. Let $\epsilon > 0$ be the largest value such that $v'_{j_1} + \frac{\epsilon}{w_{j_1}(\breve{U}_{j_1} - \breve{L}_{j_1})} \leqslant v_{j_1}$ and $v'_{j_2} - \frac{\epsilon}{w_{j_2}(\breve{U}_{j_2} - \breve{L}_{j_2})} \geqslant v_{j_2}$, and let

$$v'' \overset{\text{def}}{=} v' + \frac{\epsilon}{w_{j_1}(\breve{U}_{j_1} - \breve{L}_{j_1})}e(j_1) - \frac{\epsilon}{w_{j_2}(\breve{U}_{j_2} - \breve{L}_{j_2})}e(j_2).$$

By (26) we either have

$$\frac{x_{j_1} - \breve{L}_{j_1}}{\breve{U}_{j_1} - \breve{L}_{j_1}} = \frac{x_{j_2} - \breve{L}_{j_2}}{\breve{U}_{j_2} - \breve{L}_{j_2}} \quad \text{or} \quad \frac{x_{j_1} - \breve{L}_{j_1}}{\breve{U}_{j_1} - \breve{L}_{j_1}} < \frac{x_{j_2} - \breve{L}_{j_2}}{\breve{U}_{j_2} - \breve{L}_{j_2}}. \tag{27}$$

In the first case v'' is a feasible solution to (24) that has fewer different components with v and has the same objective value as v'. Hence, by repeating this procedure we will eventually have the second case in which v'' is a feasible solution to (24) that has an objective value strictly smaller than that of v', which contradicts the optimality of v'.

The greedy procedure to solve (7) and (24) can be executed in $\mathcal{O}(n\log(n))$ time through the sorting required to get (26). However, an optimal basic feasible solution $\hat{\alpha}$ to (24) can also be obtained in $\mathcal{O}(n)$ time by solving a weighted median problem (e.g. [21, Chapter 17.1]). This solution can be converted to an optimal solution to (7) in $\mathcal{O}(n)$ time as follows. Because $\hat{\alpha}$ is a basic feasible solution to (24), it has at most one fractional component (see, e.g., [7, Chapter 3]). Take $\hat{I} = \{\, i \in [\![n]\!] \mid \hat{\alpha}_i = 1 \,\}$. If $\hat{v}$ has one fractional component, take $\hat{h}$ to be this component. Then, because $\hat{\alpha}$ satisfies (24b) we have

$$w_{\hat{h}}(\breve{U}_{\hat{h}} - \breve{L}_{\hat{h}})\hat{\alpha}_{\hat{h}} = \sum_{i=1}^{n} w_i\breve{U}_i + b - \sum_{i \in \hat{I}} w_i(\breve{U}_i - \breve{L}_i) = \ell(\hat{I}) \tag{28}$$

Together with $\hat{\alpha}_{\hat{h}} \in (0,1)$, (25) for $I = \hat{I}$ and $h = \hat{h}$, and (23) for $i = \hat{h}$, we have $\ell(\hat{I}) > 0$ and

$$\ell(\hat{I}) - \ell(\hat{I} \cup \{\hat{h}\}) > \ell(\hat{I}).$$

Then $\ell(\hat{I} \cup \{\hat{h}\}) < 0$ and $(\hat{I}, \hat{h}) \in \mathcal{J}$. Finally, (28) implies that the objective value of $\hat{\alpha}$ for (24) is the same as the objective value of $(\hat{I}, \hat{h})$ for (7).

If, on the other hand, $\hat{v}$ has no fractional component, then $\hat{\alpha}$ satisfying (24b) implies

$$0 = \sum_{i=1}^{n} w_i\breve{U}_i + b - \sum_{i \in \hat{I}} w_i(\breve{U}_i - \breve{L}_i) = \ell(\hat{I}). \tag{29}$$

Then, $\ell(\llbracket n \rrbracket) < 0$ implies that there exists $\hat{h} \in \llbracket n \rrbracket \backslash \hat{I}$ such that $\ell(\hat{I} \cup \{\hat{h}\}) < 0$ and $(\hat{I}, \hat{h}) \in \mathcal{J}$. Finally, (29) implies that the objective value of $\hat{\alpha}$ for (24) is the same as the objective value of $(\hat{I}, \hat{h})$ for (7). This conversion of an optimal basic feasible solution for (24) to a solution to (7) also gives an alternate proof to $\omega(x) \geqslant v(x)$. □

Corollary 1. *If the weights w and biases b describing the neural network are rational, then the single-neuron relaxation* (4) *can be solved in polynomial time on the encoding sizes of w and b.*

Proof. If w and b are rational, then the coefficients of the inequalities in (6b) are also rational numbers with sizes that are polynomial in the sizes of w and b. Then the result follows from Proposition 2 and [13, Theorem 7.26]. □

C Propagation algorithms

C.1 Description and analysis of algorithms

In this section, we provide pseudocode for the propagation-based algorithms described in Section 4. In the scope of a single neuron, Algorithm 1 specifies the framework outlined in Section 4.1 and Algorithm 3 (which requires Algorithm 2) details our new algorithm proposed in Section 4.3. Finally, Algorithm 4 establishes how to compute bounds for the entire network, considering `DeepPoly` [36] and `Fast-Lin` [44] as possible initial methods.

Algorithm 1 The Backwards Pass for Upper Bounds

```
1: Inputs:
       Input domain $X \subseteq \mathbb{R}^m$, affine functions $\mathcal{L}_i(z_{1:i-1}) = \sum_{j=1}^{i-1} w^l_{ij} z_j + b^l_i$,
       $\mathcal{U}_i(z_{1:i-1}) = \sum_{j=1}^{i-1} w^u_{ij} z_j + b^u_i$ for each $i = m+1, \ldots, \eta$, and affine function
       $\mathcal{C}(z) = \sum_{i=1}^{\eta} c_i z_i + b$
2: Outputs:
       Upper bound on $\mathcal{C}(z)$, optimal point $x^* \in X$, and boolean vector
       $(\texttt{ub\_used}_{m+1}, \ldots, \texttt{ub\_used}_{\eta})$
3: function PropagationBound($X, \mathcal{L}, \mathcal{U}, \mathcal{C}$)
4:     ub_used$_i \leftarrow$ false for all $i = m+1, \ldots, \eta$
5:     $Q \leftarrow \{ i \mid c_i \neq 0, i > m \}$                ▷ Set of variable indices to be substituted
6:     expr $\leftarrow \sum_{i=1}^{\eta} c_i z_i + b$     ▷ Denote by expr.w[i] the coefficient for $z_i$ in expr, $\forall i$
7:     while $Q$ is not empty do
8:         $i \leftarrow$ pop largest value from $Q$, removing it
9:         ub_used$_i \leftarrow$ (expr.w[i] $> 0$)
10:        expr $\leftarrow$ expr $-$ expr.w[i] $z_i$                ▷ Remove term from expression
11:        if expr.w[i] $> 0$ then
12:            expr $\leftarrow$ expr $+$ expr.w[i] $\mathcal{U}_i(z_{1:i-1})$
13:            $Q \leftarrow Q \cup \{ j \mid w^u_{ij} \neq 0, j > m \}$
14:        else if expr.w[i] $< 0$ then
15:            expr $\leftarrow$ expr $+$ expr.w[i] $\mathcal{L}_i(z_{1:i-1})$
16:            $Q \leftarrow Q \cup \{ j \mid w^l_{ij} \neq 0, j > m \}$
17:        end if
18:    end while
19:    $B, x^* \leftarrow \max_{x \in X}$ expr, along with an optimal solution
20:    return $B, x^*$, ub_used
21: end function
```

Algorithm 2 The Forward Pass

```
1: Inputs:
       Partial optimal solution $x^* \in X$ from Algorithm 1 and boolean vector
       $(\texttt{ub\_used}_{m+1}, \ldots, \texttt{ub\_used}_{\eta})$ where $\texttt{ub\_used}_i = \texttt{true}$ if the upper bound $\mathcal{U}_i$
       was used to substitute variable $i$ in Algorithm 1, or false otherwise.
2: Outputs:
       Optimal solution $z^*_{1:\eta}$ to (9)
3: function RecoverCompleteSolution($x^*$, ub_used)
4:     $z^*_i = x^*_i$ for $i = 1, \ldots, m$
5:     for $i = m+1, \ldots, \eta$ do
6:         if $\texttt{ub\_used}_i = \texttt{true}$ then
7:             $z^*_i \leftarrow \mathcal{U}_i(z^*_{1:i-1})$
8:         else
9:             $z^*_i \leftarrow \mathcal{L}_i(z^*_{1:i-1})$
10:        end if
11:    end for
12:    return $z^*_{1:\eta}$
13: end function
```

Algorithm 3 The Iterative Algorithm

```
1: Inputs:
       Input domain $X \subseteq \mathbb{R}^m$, initial affine bounding functions $\{\mathcal{L}_i^{\text{init}}\}_{i=m+1}^{\eta}$,
       $\{\mathcal{U}_i^{\text{init}}\}_{i=m+1}^{\eta}$, affine function $\mathcal{C}: \mathbb{R}^{\eta} \to \mathbb{R}$, and number of iterations $T \geqslant 0$
2: Outputs:
       An upper bound on $\max_{x \in X} \mathcal{C}(x)$
3: function TightenedPropagationBound($X, \mathcal{L}, \mathcal{U}, \mathcal{C}, k$)
4:     $\{\mathcal{L}_i, \mathcal{U}_i\}_{i=m+1}^{\eta} \leftarrow \{\mathcal{L}_i^{\text{init}}, \mathcal{U}_i^{\text{init}}\}_{i=m+1}^{\eta}$
5:     $B, x^*, \texttt{ub\_used} \leftarrow$ PropagationBound($X, \{\mathcal{L}_i\}_{i=m+1}^{\eta}, \{\mathcal{U}_i\}_{i=m+1}^{\eta}, \mathcal{C}$)
6:     for $\texttt{iter} = 1, \ldots, T$ do
7:         $z^*_{1:\eta} \leftarrow$ RecoverCompleteSolution($x^*$, ub_used)
8:         for $i = m+1, \ldots, \eta$ do
9:             $\mathcal{U}_i', v \leftarrow$ most violated inequality w.r.t. $z^*_{1:\eta}$ from (6b) (per Prop. 2) and its violation
10:            if $v > 0$ then $\mathcal{U}_i \leftarrow \mathcal{U}_i'$ end if
11:        end for
12:        $B', x^*, \texttt{ub\_used} \leftarrow$ PropagationBound($X, \{\mathcal{L}_i\}_{i=m+1}^{\eta}, \{\mathcal{U}_i\}_{i=m+1}^{\eta}, \mathcal{C}$)
13:        if $B' < B$ then $B \leftarrow B'$ end if
14:    end for
15:    return $B$
16: end function
```

Proposition 4. *The solution z^* returned by Algorithm 2 is optimal for the relaxed problem* (9).

Proof. Denote by $\texttt{expr}^k \overset{\text{def}}{=} \sum_{j \in J^k} \texttt{w}_j^k z_j + \texttt{b}^k$ the expression expr at the end of iteration $k = 1, \ldots, K$ of the while loop in Algorithm 1, for some subsets $J^1, \ldots, J^K \subseteq [\![\eta]\!]$, and let $\texttt{expr}^0$ be the initial expr as defined in line 5, i.e. $\mathcal{C}(z)$. For each $k = 0, \ldots, K-1$, we obtain $\texttt{expr}^{k+1}$ by replacing, for some i, z_i by $\mathcal{U}_i(z_{1:i-1})$ if $\texttt{w}_i^k > 0$, or by $\mathcal{L}_i(z_{1:i-1})$ if if $\texttt{w}_i^k < 0$. Note that if $\texttt{w}_i^k = 0$, we can safely ignore any substitution because it will not affect the expression. Due to the constraints (9c), this substitution implies that $\texttt{expr}^k \leqslant \texttt{expr}^{k+1}$ for any $z_{1:m} \in X$. This inductively establishes that, restricting to $z_{1:m} \in X$,

$$\mathcal{C}(z) = \sum_{j=1}^{\eta} c_j z_j + b \leqslant \sum_{j \in J^1} \texttt{w}_j^1 z_j + \texttt{b}^1 \leqslant \ldots \leqslant \sum_{j \in J^K} \texttt{w}_j^K z_j + \texttt{b}^K, \tag{30}$$

Note that $J^K \subseteq \{z_1, \ldots, z_m\}$ since we have made all the substitutions possible for $i > m$. Therefore, the optimal value of (9) is upper-bounded by the bound corresponding to the solution returned by

Algorithm 4 `FastC2V` Algorithm

```
1: Inputs:
       A feedforward neural network as defined in (1) (with input domain $X$, ReLU
       neurons $i = m+1, \ldots, N$, and a single affine output neuron indexed by $N+1$),
       initial_method $\in$ {DeepPoly, Fast-Lin}, and number of iterations per
       neuron $T \geqslant 0$ (note that if $T = 0$, we recover DeepPoly or Fast-Lin)
2: Outputs:
       Lower and upper bounds $\{\hat{L}_i, \hat{U}_i\}_{i=1}^{N+1}$ on the pre-activation function (if ReLU) or
       output (if affine) of neuron $i$
3: function FastC2V($X, W, b,$ initial_method$, T$)
4:     for $i = m+1, \ldots, N+1$ do
5:         $\mathcal{C}(z_{1:i-1}) \leftarrow \sum_{j=1}^{i-1} w_{i,j} z_j + b_i$
6:         $\hat{L}_i \leftarrow -$ TightenedPropagationBound($X, \{\mathcal{L}_j\}_{j=m+1}^{i-1}, \{\mathcal{U}_j\}_{j=m+1}^{i-1}, -\mathcal{C}, T$)
7:         $\hat{U}_i \leftarrow$ TightenedPropagationBound($X, \{\mathcal{L}_j\}_{j=m+1}^{i-1}, \{\mathcal{U}_j\}_{j=m+1}^{i-1}, \mathcal{C}, T$)
8:         if $i = N+1$ then break end if
9:         ▷ Build bounding functions $\mathcal{L}_i$ and $\mathcal{U}_i$ for subsequent iterations
10:        if $\hat{L}_i \geqslant 0$ then                    ▷ ReLU $i$ is always active for any $z_{1:m} \in X$
11:            $\mathcal{L}_i(z_{1:i-1}) \leftarrow \sum_{j=1}^{i-1} w_{i,j} z_j + b_i$
12:            $\mathcal{U}_i(z_{1:i-1}) \leftarrow \sum_{j=1}^{i-1} w_{i,j} z_j + b_i$
13:        else if $\hat{U}_i \leqslant 0$ then               ▷ ReLU $i$ is always inactive for any $z_{1:m} \in X$
14:            $\mathcal{L}_i(z_{1:i-1}) \leftarrow 0$
15:            $\mathcal{U}_i(z_{1:i-1}) \leftarrow 0$
16:        else
17:            $\mathcal{U}_i(z_{1:i-1}) \leftarrow \frac{\hat{U}_i}{\hat{U}_i - \hat{L}_i}(\sum_{j=1}^{i-1} w_{i,j} z_j + b_i - \hat{L}_i)$
18:            if initial_method = DeepPoly then
19:                if $|\hat{L}_i| \geqslant |\hat{U}_i|$ then $\mathcal{L}_i(z_{1:i-1}) \leftarrow 0$ else $\mathcal{L}_i(z_{1:i-1}) \leftarrow \sum_{j=1}^{i-1} w_{i,j} z_j + b_i$ end if
20:            else   ▷ initial_method = Fast-Lin
21:                $\mathcal{L}_i(z_{1:i-1}) \leftarrow \frac{\hat{U}_i}{\hat{U}_i - \hat{L}_i}(\sum_{j=1}^{i-1} w_{i,j} z_j + b_i)$
22:            end if
23:        end if
24:    end for
25:    return $\{\hat{L}_i, \hat{U}_i\}_{i=1}^{N+1}$
26: end function
```

Algorithm 1, that is,

$$\max \{ \mathcal{C}(z) \mid z_{1:m} \in X, \text{ (9c)} \} \leqslant \max \left\{ \sum_{j \in J^K} \mathtt{w}_j^K z_j + \mathtt{b}^K \;\middle|\; z_{1:m} \in X \right\}.$$

To see that this upper bound is achieved, observe that each inequality in (30) holds as equality if we substitute $z_j = z_j^*$ for all j, by construction of Algorithm 2 and boolean vector $(\mathtt{ub\_used}_{m+1}, \ldots, \mathtt{ub\_used}_\eta)$. Note also that z^* satisfies (9c) by construction. That is, we have a feasible z^* such that $\mathcal{C}(z^*)$ is no less than the optimal value of (9), and thus z^* must be an optimal solution. □

We would like to highlight to the interested reader that this result can also be derived from an argument using Fourier-Motzkin elimination [7, Chapter 2.8] to project out the intermediate variables $z_{m+1:\eta}$. Notably, as each inequality neuron has exactly one inequality upper bounding and one inequality lower bounding its post-activation value, this projection does not produce an "explosion" of new inequalities as is typically observed when applying Fourier-Motzkin to an arbitrary polyhedron.

Define $C \overset{\text{def}}{=} |\{ i \in [\![\eta]\!] \mid c_i \neq 0 \}|$ and suppose that we use the affine bounding inequalities from `Fast-Lin` or `DeepPoly`. Let T be the number of iterations in Algorithm 3, $opt(X)$ be the time required to maximize an arbitrary affine function over X, and A be the number of arcs in the network (i.e. nonzero weights).

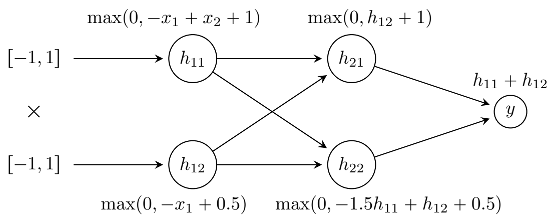

(a) Structure and weights of the example network.

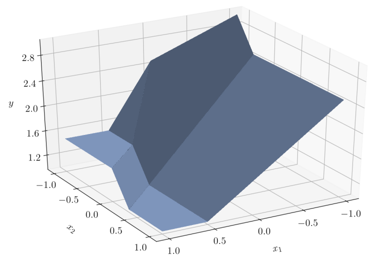

(b) Output of the example network (rotated).

Figure 4: An example network with 4 ReLUs on which we simulate `FastC2V`.

Observation 1. *Algorithm 1 runs in $opt(X) + \mathcal{O}(C + A)$ time. Algorithm 2 runs in $\mathcal{O}(A)$ time. Algorithm 3 runs in $(T + 1)opt(X) + \mathcal{O}(T(C + A))$ time.*

Observation 2. *Algorithm 4 takes $\mathcal{O}(NT(opt(X) + A))$ time if $T \geqslant 1$. If $T = 0$, then Algorithm 4 takes $\mathcal{O}(N(opt(X) + A))$ time.*

C.2 Proofs of other results from section 4

Proposition 3. *The optimal value of* (9) *is no less than* $\max_{x \in X} \mathcal{C}\left(z_{1:\eta}\left(x\right)\right)$.

Proof. For any $x \in X$, by definition of validity in (8), setting $z_i \leftarrow z_i(x)$ for all $i = 1, \ldots, N$ yields a feasible solution to (9) with objective value $c\left(z_{1:N}\left(x\right)\right)$, completing the proof. $\square$

D An example for `FastC2V`

In this section, we walk through the `FastC2V` algorithm step-by-step for the following $\mathbb{R}^2 \to \mathbb{R}$ network with four ReLUs, also illustrated in Figure 4:

$$\begin{aligned}
x_1 &\in [-1, 1] \\
x_2 &\in [-1, 1] \\
h_{11} &= \max(0, -x_1 + x_2 + 1) \\
h_{12} &= \max(0, -x_1 + 0.5) \\
h_{21} &= \max(0, h_{12} + 1) \\
h_{22} &= \max(0, -1.5h_{11} + h_{12} + 0.5) \\
y &= h_{21} + h_{22}
\end{aligned}$$

Our goal is to compute an upper bound for y using `FastC2V`.

Our procedure requires lower and upper bounds for each pre-activation function, and this can be obtained by running the same algorithm for each neuron, layer by layer. For simplicity, in this example we start from bounds computed via interval arithmetic.

Denote by $\hat{h}_{ij}$ the pre-activation function of h_{ij}. To apply interval arithmetic, we simply substitute the variables by their lower or upper bounds as to minimize or maximize them (applying the ReLU activation function when needed). For example, the interval arithmetic upper bound of $\hat{h}_{11}$ is $-1.5 \times (-1) + 1 + 0.5 = 3$. Starting at $x_1 \in [-1, 1]$ and $x_2 \in [-1, 1]$, we have:

$$\begin{aligned}
&\hat{h}_{11} \in [-1, 3] \quad (h_{11} \in [0, 3]) \qquad &&\hat{h}_{21} \in [1, 2.5] \quad (h_{21} \in [1, 2.5]) \\
&\hat{h}_{12} \in [-0.5, 1.5] \quad (h_{12} \in [0, 1.5]) \qquad &&\hat{h}_{22} \in [-4, 2] \quad (h_{22} \in [0, 2])
\end{aligned}$$

Note that $\hat{h}_{21} \geqslant 0$ for any input $x \in [-1, 1]^2$, and thus we may infer that the ReLU will always be active. That is, we can assume $h_{21} = h_{12} + 1$. This linearization step not only can have a large impact in bound strength, but also is required for correctness, as the formulations assume that the lower bound is negative and the upper bound positive.

Therefore, we drop h_{21} altogether and set

$$y = h_{12} + h_{22} + 1.$$

Observe that interval arithmetic already gives us a simple upper bound on y of 4.5.

We begin by applying `DeepPoly` [36] (or `CROWN-Ada` [49]), following Algorithm 1. Consider briefly a ReLU $y = \max(0, w^\top x + b)$ with pre-activation bounds $[\hat{L}, \hat{U}]$. In `DeepPoly`, we select the lower bounding inequality to be $y \geqslant 0$ if $|\hat{L}| \geqslant |\hat{U}|$, or $y \geqslant w^\top x + b$ otherwise. The upper bounding inequality comes from the Δ-relaxation and can be expressed as $y \leqslant \frac{\hat{U}}{\hat{U}-\hat{L}}(w^\top x + b - \hat{L})$. Thus, based on the previously computed bounds, we have:

$$\begin{aligned}
-x_1 + x_2 + 1 \leqslant h_{11} &\leqslant -\frac{3}{4}x_1 + \frac{3}{4}x_2 + \frac{3}{2} \\
-x_1 + \frac{1}{2} \leqslant h_{12} &\leqslant -\frac{3}{4}x_1 + \frac{3}{4} \\
0 \leqslant h_{22} &\leqslant -\frac{1}{2}h_{11} + \frac{1}{3}h_{12} + \frac{3}{2}
\end{aligned}$$

The next step is to maximize y over the relaxation given by the above inequalities plus bounds (including on the input). We replace variables with the above bounding inequalities, layer by layer. Since we are maximizing, we use the upper bounding inequality if the corresponding coefficient is positive, or the lower bound inequality otherwise. This maintains validity of the inequality throughout the process.

$$\begin{aligned}
y = h_{12} + h_{22} + 1 &\leqslant h_{12} + \left(-\frac{1}{2}h_{11} + \frac{1}{3}h_{12} + \frac{3}{2}\right) + 1 \\
&= -\frac{1}{2}h_{11} + \frac{4}{3}h_{12} + \frac{5}{2} \\
&\leqslant -\frac{1}{2}\left(-x_1 + x_2 + 1\right) + \frac{4}{3}\left(-\frac{3}{4}x_1 + \frac{3}{4}\right) + \frac{5}{2} \\
&= -\frac{1}{2}x_1 - \frac{1}{2}x_2 + 3
\end{aligned}$$

Now that we have inferred the above upper bounding inequality on y, we convert it into an upper bound by solving the simple problem $\max_{x \in [-1,1]^2} -\frac{1}{2}x_1 - \frac{1}{2}x_2 + 3$, which yields 4, with an optimal solution $(-1, -1)$. This is the resulting upper bound from the `DeepPoly` algorithm.

We next show how to tighten it with `FastC2V`. The first step is to recover an actual optimal solution of the relaxation above. This is the forward pass described in Algorithm 2.

We first make note that we used the upper bounding inequality for h_{12} and h_{22} and the lower bounding inequality for h_{11}. We start from the optimal solution in the input space, $(-1, -1)$, and recover values for each h_{ij} and y according to the bounding inequalities used, considering them to be equalities. For example, $h_{11} = -(-1) + (-1) + 1 = 1$. The result is the solution $\bar{p} = (-1, -1, 1, 1.5, 1.5, 4)$ in the $(x_1, x_2, h_{11}, h_{12}, h_{22}, y)$-space.

We now perform the main step of `FastC2V`, which is to swap upper bounding inequalities based on p. They are swapped to whichever inequality is violated by p, or not swapped if no inequality is violated for a given ReLU neuron.

In this example, we skip h_{11} and h_{12} for simplicity as no swapping occurs, and we focus on h_{22}. For h_{22}, the relevant values of $\bar{p}$ are $\bar{h}_{11} = 1$, $\bar{h}_{12} = 1.5$, and $\bar{h}_{22} = 1.5$. Normally, we would solve the separation problem at this point, but for illustrative purposes we list out all possible upper bounding inequalities that we can swap to.

Recall Theorem 1 and compute:

$$\begin{aligned}
\ell(\varnothing) &= 2 & \qquad \ell(\{1\}) &= -2.5 \\
\ell(\{2\}) &= 0.5 & \qquad \ell(\{1,2\}) &= -4
\end{aligned}$$

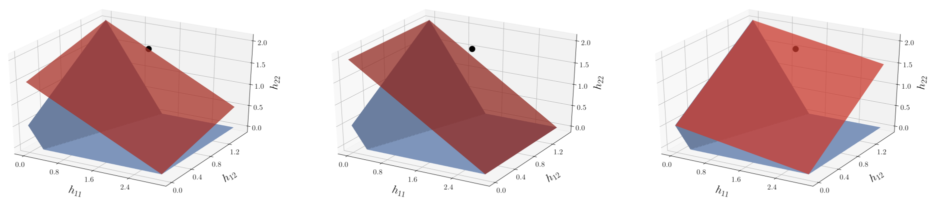

(a) Original inequality from the Δ-relaxation.

(b) Inequality (31).

(c) Inequality (32).

Figure 5: Three options of upper bounding inequalities for h_{22}. The black point depicts the solution that we would like to separate, which is cut off by inequality (31).

Based on these values, we have $\mathcal{J} = \{(\varnothing, 1), (\{2\}, 1)\}$, or in other words, two possible inequalities to swap to. By following the formulation in Theorem 1, we obtain the inequalities

$$h_{22} \leqslant -\frac{2}{3}h_{11} + 2 \tag{31}$$

$$h_{22} \leqslant -\frac{1}{6}h_{11} + h_{12} + \frac{1}{2} \tag{32}$$

These inequalities are illustrated in Figure 5. We observe that our point p is cut off by the inequality (31): $1.5 = \bar{h}_{22} > -\frac{2}{3}\bar{h}_{11} + 2 = \frac{4}{3} \approx 1.333$. Therefore, for this neuron, we swap the upper bounding inequality to (31). In other words, our pair of inequalities for h_{22} is now:

$$0 \leqslant h_{22} \leqslant -\frac{2}{3}h_{11} + 2$$

The last step of `FastC2V` is to redo the backward propagation with the swapped inequalities and recompute the bound. We obtain:

$$\begin{aligned} y = h_{12} + h_{22} + 1 &\leqslant h_{12} + \left(-\frac{2}{3}h_{11} + 2\right) + 1 \\ &= -\frac{2}{3}h_{11} + h_{12} + 3 \\ &\leqslant -\frac{2}{3}\left(-x_1 + x_2 + 1\right) + \left(-\frac{3}{4}x_1 + \frac{3}{4}\right) + 3 \\ &= -\frac{1}{12}x_1 - \frac{2}{3}x_2 + \frac{37}{12} \end{aligned}$$

Solving $\max_{x\in[-1,1]^2} -\frac{1}{12}x_1 - \frac{2}{3}x_2 + \frac{37}{12}$ gives us an improved bound of $\frac{23}{6} \approx 3.833$, completing the `FastC2V` algorithm for upper bounding y. Note that this procedure is not guaranteed to improve the initial bound, and in general we take the best between the initial bound and the new one.

Incidentally, we observe in Figure 5(a) that the big-M inequality from the Δ-relaxation is, in general, not facet-defining for the convex hull of the feasible points depicted in blue. This explains why it can not be directly reconstructed from our convex hull description (6).

E Implementation details

In this section, we add to the implementation details provided in Section 5.

The implementation of the propagation-based algorithm involves the following details:

- It may occur that the result of Algorithm 1 has zero coefficients for some variables x_i, in which case any feasible value for x_i produces an optimal solution. For those variables, we select the midpoint between the lower bound and upper bound to proceed with Algorithm 2.

- We find that running more than one iteration of the propagation-based algorithm does not yield improving results. A possible reason for this is that while these inequalities are stronger in some portions of the input space, they are looser by themselves in others, and balancing this can be difficult. Improving this trade-off however is outside the scope of this paper.
- We use no tolerance on violation. That is, every violated inequality is swapped in.

The implementation of the LP-based algorithm involves the following details:

- We find that the Conv networks examined are very numerically unstable for LPs due to the presence of very small weights in the networks. Taking no action results in imprecise solutions, sometimes resulting in infeasible LPs being constructed. To improve on this instability, we consider as zero any weight or generated bound below 10^{-5}. In addition, we run `DeepPoly` before the LP to quickly check if the neuron can be linearized. This is applied only to the LP-based methods. Note that the default feasibility and optimality tolerances in Gurobi are 10^{-6}. With this, we end up solving an approximate problem rather than the exact problem, though arguably it is too difficult to solve these numerically unstable LPs with high precision and reasonable time in practice.
- For separation, we implement the $O(n \log n)$ version of the algorithm based on sorting instead of the $O(n)$ version.
- For each bound computed, we generate new cuts from scratch. More specifically, when solving for each bound, we make a copy of the model and its LP basis from the previous solve, run the LP solve and cut loop, retrieve the bound, and then discard this copy of the model.
- We add cuts whose violation exceeds a tolerance of 10^{-5}.
- In the context of mixed-integer programming, it is well known that selecting a smaller subset of cuts to add can be very beneficial to reduce solving time, but for simplicity, we perform no cut selection in this method.
- An alternative to the LP-based method is to solve a MIP with analogous cutting planes with binary variables [3], but we find that this method, free of binary variables, is more lightweight and effective even without cut selection and all the presolve functionalities of modern MIP solvers. The ability to solve these LPs very quickly is important since we solve them at every neuron. In addition, this gives us more fine-grained control on the cuts, providing a better opportunity to evaluate our inequalities.

The implementation of all algorithms involve the following details:

- We attempt to linearize each neuron with simple interval arithmetic before running a more expensive procedure. This makes a particularly large difference in solving time for the Conv networks, in which many neurons are linearizable.
- As done in other algorithms in the literature, we elide the last affine layer, a step that is naturally incorporated in the framework from Section 4.1. In other words, we do not consider the last affine layer to be a neuron but to be the objective function.
- We fully compute the bounds of all neurons in the network, including differences of logits. We make no attempt to stop early even if we have the opportunity to infer robustness earlier.
- When solving the verification problem, scalar bounds on the intermediate neurons only need to be computed once per input image (i.e. once per set X), and can be reused for each target class (i.e. reused for different objectives c).

The details of the networks from the ERAN dataset [38] are the following. To simplify notation, we denote a dense layer by `Dense(size, activation)` and a convolutional layer by `Conv2D(number of filters, kernel size, strides, padding, activation)`.

- 6x100: $5\times$ `Dense(100, ReLU)` followed by `Dense(10, ReLU)`. This totals 510 units. Trained on the MNIST dataset with no adversarial training.
- 9x100: $8\times$ `Dense(100, ReLU)` followed by `Dense(10, ReLU)`. This totals 810 units. Trained on the MNIST dataset with no adversarial training.

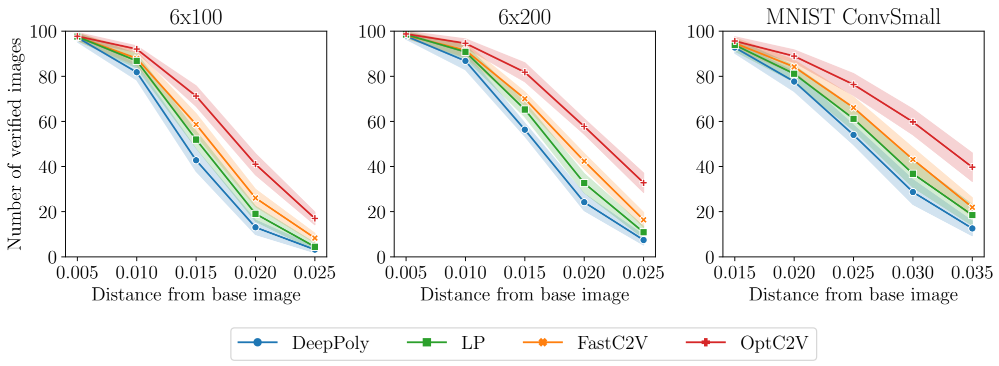

Figure 6: Number of verified images by each method given various values of the allowed distance from the base image. Lines are averages over 16 randomly initialized networks and error bands represent standard deviation.

- 6x200: 5× `Dense(200, ReLU)` followed by `Dense(10, ReLU)`. This totals 1010 units. Trained on the MNIST dataset with no adversarial training.
- 6x200: 8× `Dense(200, ReLU)` followed by `Dense(10, ReLU)`. This totals 1610 units. Trained on the MNIST dataset with no adversarial training.
- MNIST ConvSmall: `Conv2D(16, (4,4), (2,2), valid, ReLU)`, `Conv2D(32, (4,4), (2,2), valid, ReLU)`, `Dense(100, ReLU)`, `Dense(10, linear)`. This totals 3604 units. Trained on the MNIST dataset with no adversarial training.
- MNIST ConvBig: `Conv2D(32, (3,3), (1,1), same, ReLU)`, `Conv2D(32, (4,4), (2,2), same, ReLU)`, `Conv2D(64, (3,3), (1,1), same, ReLU)`, `Conv2D(64, (4,4), (2,2), same, ReLU)`, `Dense(512, ReLU)`, `Dense(512, ReLU)`, `Dense(10, linear)`. This totals 48064 units. Trained on the MNIST dataset with DiffAI for adversarial training.
- CIFAR-10 ConvSmall: `Conv2D(16, (4,4), (2,2), valid, ReLU)`, `Conv2D(32, (4,4), (2,2), valid, ReLU)`, `Dense(100, ReLU)`, `Dense(10, linear)`. This totals 4852 units. Trained on the CIFAR-10 dataset with projected gradient descent for adversarial training.

F Supplementary computational results

We computationally examine the sensitivity of the algorithms in this paper to different training initializations and distances from the base image.

We focus on networks for the MNIST dataset. The first two architectures 6x100 and 6x200 have 6 hidden layers of 100 and 200 ReLUs respectively, followed by a linear output layer of 10 ReLUs (this differs slightly from the ERAN networks of the same name described in Appendix E). The MNIST ConvSmall architecture is the same as described in Appendix E. Average test accuracies are 97.04%, 97.61%, and 98.63% respectively. For each architecture and distance, we train 16 randomly initialized networks. Each network is trained with a learning rate of 0.001 for 10 epochs using the Adam training algorithm, without any adversarial training.

Figure 6 illustrates the average number of verified images. The error bands represent standard deviation over the 16 networks. We observe that OptC2V and FastC2V perform well across different networks and distances.

In addition, Figure 7 depicts survival plots for the results from Table 1: the number of images that can be verified given individual time budgets.

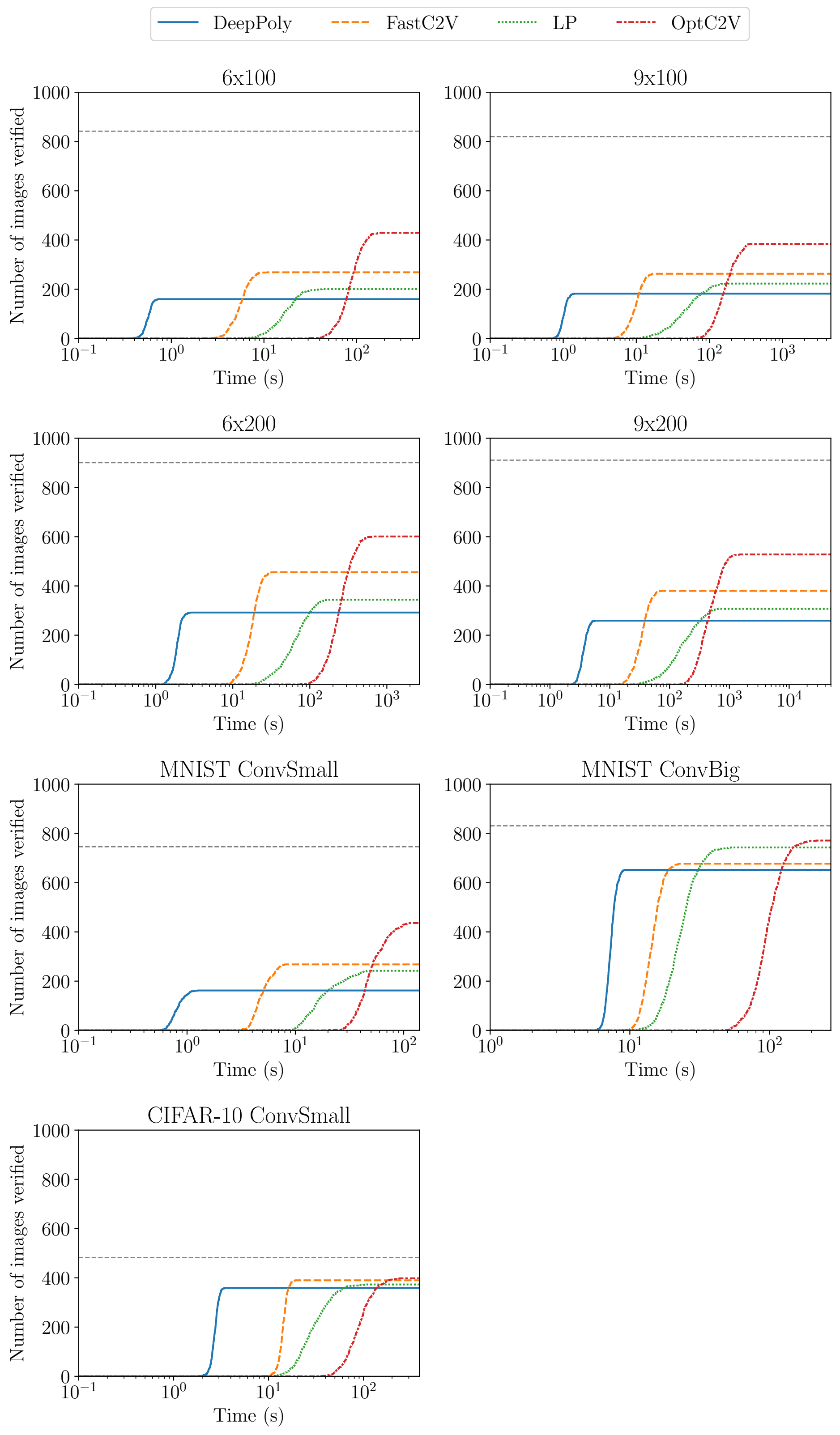

Figure 7: Survival plots for the results in Section 5. The horizontal dashed line is the upper bound on the number of verifiable images.